A 3D visualization of a particle simulation. The background is dark blue with a dense field of yellow particles. A prominent, jagged blue structure, possibly a shock front or a filament, extends diagonally across the scene. In the lower-left foreground, there is a large, multi-colored volume (purple, green, red) also filled with particles. An orange horizontal bar is located in the top-left corner.

# Particle methods for laser-produced plasmas

---

doc. Ing. Ondřej Klimo, Ph.D.  
FJFI CTU in Prague, ELI ERIC  
[ondrej.klimo@fjfi.cvut.cz](mailto:ondrej.klimo@fjfi.cvut.cz)



## Outline

What is unique about laser plasma modelling?

- Strong electromagnetic fields
- Relativistic particle dynamics
- Radiation and QED effects – lect. 5
- Field ionization
- Coulomb collisions

Numerical aspects (boundary conditions, numerical Cherenkov radiation)

Advanced features (envelope approximation, boost/moving frame)

Codes

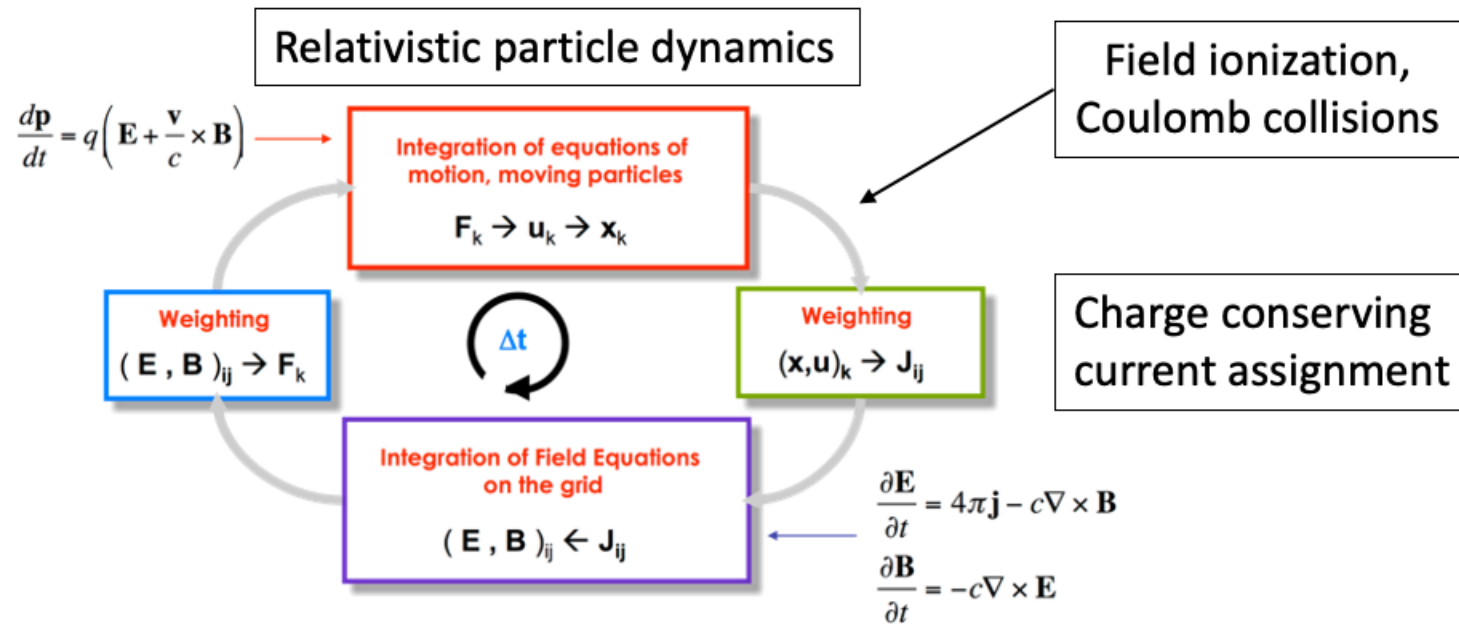
Examples

# Particle methods for laser-produced plasmas

Simulation techniques  
in hot plasma modeling

## Core PIC algorithm

- The core of a Particle-in-Cell code is two coupled solvers:
  - Meshless charged particles dynamics under the influence of EM fields
  - Time evolution of EM fields on a fixed spatial grid



## EM fields – Maxwell's equations

- Recall microscopic version of Maxwell's equations before discussing their solution

In the microscopic version the material medium is not built into the structure of the equations but appears only in the charge and current terms.

- Gauss's law (Poisson eq.)

$$\nabla \cdot \mathbf{E} = \frac{\rho}{\epsilon_0}$$

- Gauss's law for magnetism

$$\nabla \cdot \mathbf{B} = 0$$

- Faraday's law

$$\nabla \times \mathbf{E} = -\frac{\partial \mathbf{B}}{\partial t}$$

- Ampere's law

$$\nabla \times \mathbf{B} = \mu_0 \mathbf{J} + \mu_0 \epsilon_0 \frac{\partial \mathbf{E}}{\partial t}$$

- These 4 equations are not necessary.
  - Taking divergence of Ampere's law and assuming charge conservation – Gauss's law.
  - Similarly for Faraday's law and Gauss's law for magnetism.



### EM fields – FDTD

- **Finite-difference time-domain method (FDTD)** one of the most popular computational methods for electromagnetic problems
- Proposed by Dr. K. S. Yee in 1966
- Simple, efficient and easily adaptable, explicit in the time step
- **E, B fields are discretized on staggered Yee's grid**
- Using centered differences in time and space second order accuracy
- Discretized equations are

$$\mathbf{E}^{(n+1)} = \mathbf{E}^{(n)} + \Delta t \left[ (\nabla \times \mathbf{B})^{(n+\frac{1}{2})} - \mathbf{J}^{(n+\frac{1}{2})} \right]$$

$$\mathbf{B}^{(n+\frac{3}{2})} = \mathbf{B}^{(n+\frac{1}{2})} - \Delta t (\nabla \times \mathbf{E})^{(n+1)}$$

#### Numerical Solution of Initial Boundary Value Problems Involving Maxwell's Equations in Isotropic Media

KANE S. YEE

*Abstract*—Maxwell's equations are replaced by a set of finite difference equations. It is shown that if one chooses the field points appropriately, the set of finite difference equations is applicable for a boundary condition involving perfectly conducting surfaces. An example is given of the scattering of an electromagnetic pulse by a perfectly conducting cylinder.

obstacle is moderately large compared to that of an incoming wave.

A set of finite difference equations for the system of partial differential equations will be introduced in the early part of this paper. We shall then show that with an appropriate choice of the points at which the various

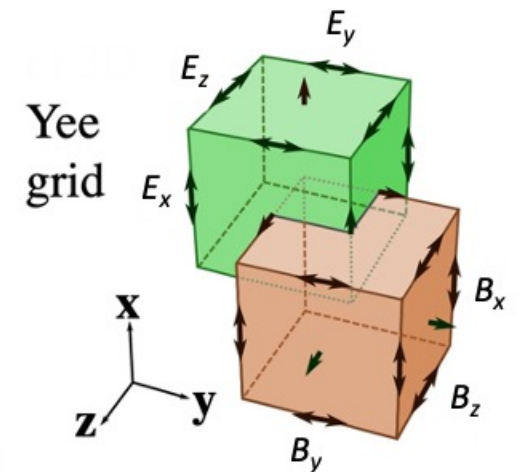
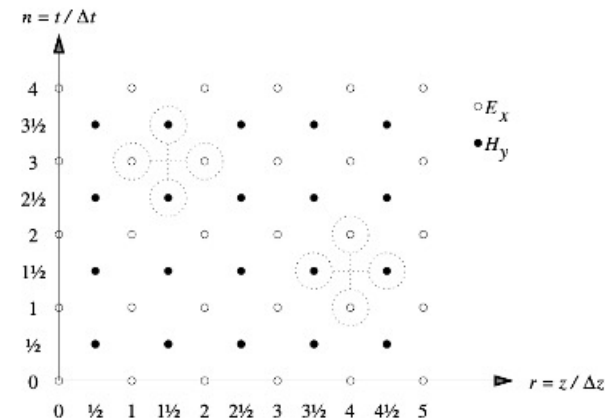


Fig. 5.8. Staggered grid used in the 1D leap-frog algorithm. The two "stencils" show which values of  $E_x$  and  $H_y$  are used in solving (5.13) with  $(r = 1, n = 3)$  and in solving (5.12) with  $(r = 4, n = 1)$ .

## EM fields – FDTD – stability

- Stability analysis of the centered difference scheme using wave equation in vacuum and plane EM wave

$$\nabla^2 \mathbf{E} - \frac{1}{c^2} \frac{\partial^2 \mathbf{E}}{\partial t^2} = 0 \quad \mathbf{E} = \mathbf{E}_0 \exp(i\omega t - i\mathbf{k}\mathbf{r})$$

$$\frac{e^{-ik_x \Delta x} - 2 + e^{+ik_x \Delta x}}{\Delta x^2} + \frac{e^{-ik_y \Delta y} - 2 + e^{+ik_y \Delta y}}{\Delta y^2} + \frac{e^{-ik_z \Delta z} - 2 + e^{+ik_z \Delta z}}{\Delta z^2} = \frac{e^{-i\omega \Delta t} - 2 + e^{+i\omega \Delta t}}{c^2 \Delta t^2}$$

**3D**

$$\frac{\sin^2(k_x \Delta x / 2)}{(\Delta x)^2} + \frac{\sin^2(k_y \Delta y / 2)}{(\Delta y)^2} + \frac{\sin^2(k_z \Delta z / 2)}{(\Delta z)^2} = \frac{\sin^2(\omega \Delta t / 2)}{(c \Delta t)^2}$$

**Courant Fridrich Levy (CFL) stability condition**

$$\Delta t \leq \frac{1}{c} \frac{1}{\sqrt{\frac{1}{\Delta x^2} + \frac{1}{\Delta y^2} + \frac{1}{\Delta z^2}}}$$

**1D**

$$\sin^2(k_x \Delta x / 2) = \left( \frac{\Delta x}{c \Delta t} \right)^2 \sin^2(\omega \Delta t / 2)$$

**CFL stability condition**

$$\Delta t \leq \frac{1}{c} \frac{1}{\sqrt{\frac{1}{\Delta x^2}}} = \frac{\Delta x}{c}$$

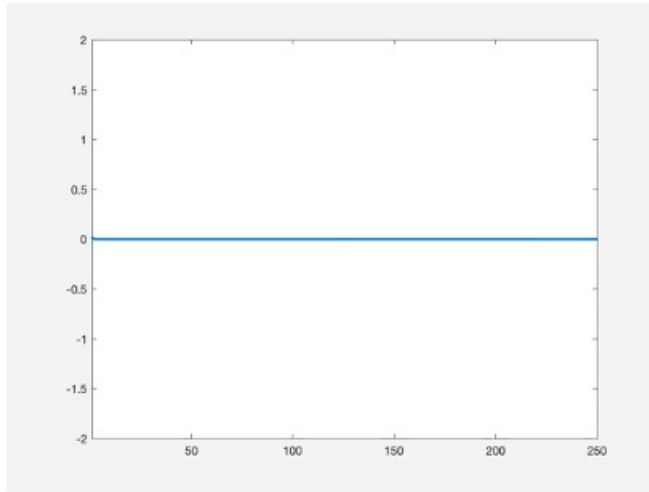


# Particle methods for laser-produced plasmas

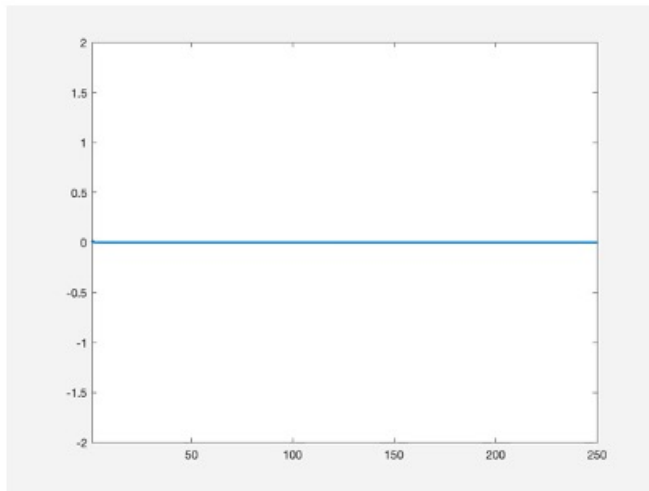
## EM fields – FDTD – numerical dispersion properties

## Simulation techniques in hot plasma modeling

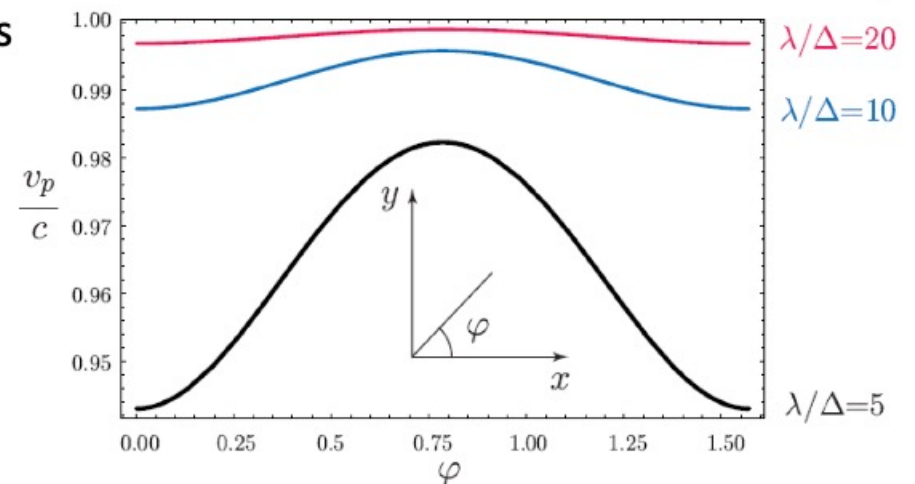
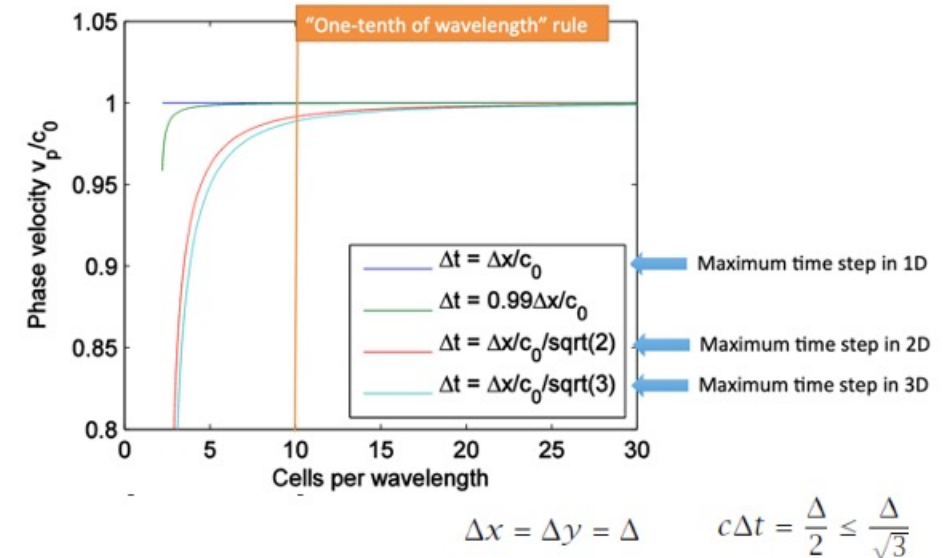
dispersion  
 $c\Delta t < \Delta x$



instability  
 $c\Delta t > \Delta x$



Dispersion properties  
versus numerical  
resolution and angle  
of propagation with  
respect to the grid axis



- Three main types of boundary conditions
  - perfect electric conductor - mimics a perfect metal surface reflecting all EM waves
  - periodic boundary conditions emulate a periodic continuation of the domain
  - **absorbing boundary conditions (ABC)** simulate open systems
- ABC - dissipation within an absorbing boundary layer without reflection
- Achieved using Maxwell's curl equations for a dissipative medium

$$\sigma_x(x) = \left(\frac{x}{d}\right)^m \sigma_{x,\max}$$

$$\begin{aligned} \nabla \times \mathbf{H} &= \frac{\partial \mathbf{D}}{\partial t} + \sigma \mathbf{E}, & \mathbf{D} &= \epsilon_0 \epsilon_r \mathbf{E} = \epsilon \mathbf{E}, \\ \nabla \times \mathbf{E} &= -\frac{\partial \mathbf{B}}{\partial t} - \sigma^* \mathbf{H}, & \mathbf{B} &= \mu_0 \mu_r \mathbf{H} = \mu \mathbf{H} \end{aligned}$$

- Uniaxial perfectly matched layer (UPML) achieve perfect matching at the interface via an uniaxial anisotropic absorption layer

$$\begin{aligned} \frac{\partial D_x}{\partial t} &= \left[ \frac{\partial H_z}{\partial y} - \frac{\partial H_y}{\partial z} - \frac{\sigma_y}{\epsilon} D_x \right], & \frac{\partial}{\partial t} D_x + \frac{\sigma_x}{\epsilon} D_x &= \epsilon \left[ \frac{\partial}{\partial t} E_x + \frac{\sigma_z}{\epsilon} E_x \right] \\ \frac{\partial D_y}{\partial t} &= \left[ \frac{\partial H_x}{\partial z} - \frac{\partial H_z}{\partial x} - \frac{\sigma_z}{\epsilon} D_y \right], & \frac{\partial}{\partial t} D_y + \frac{\sigma_y}{\epsilon} D_y &= \epsilon \left[ \frac{\partial}{\partial t} E_y + \frac{\sigma_x}{\epsilon} E_y \right] \\ \frac{\partial D_z}{\partial t} &= \left[ \frac{\partial H_y}{\partial x} - \frac{\partial H_x}{\partial y} - \frac{\sigma_x}{\epsilon} D_z \right], & \frac{\partial}{\partial t} D_z + \frac{\sigma_z}{\epsilon} D_z &= \epsilon \left[ \frac{\partial}{\partial t} E_z + \frac{\sigma_y}{\epsilon} E_z \right] \\ \frac{\partial B_x}{\partial t} &= \left[ \frac{\partial E_y}{\partial z} - \frac{\partial E_z}{\partial y} - \frac{\sigma_y}{\epsilon} B_x \right], & \frac{\partial}{\partial t} B_x + \frac{\sigma_x}{\epsilon} B_x &= \mu \left[ \frac{\partial}{\partial t} H_x + \frac{\sigma_z}{\epsilon} H_x \right] \\ \frac{\partial B_y}{\partial t} &= \left[ \frac{\partial E_z}{\partial x} - \frac{\partial E_x}{\partial z} - \frac{\sigma_z}{\epsilon} B_y \right], & \frac{\partial}{\partial t} B_y + \frac{\sigma_y}{\epsilon} B_y &= \mu \left[ \frac{\partial}{\partial t} H_y + \frac{\sigma_x}{\epsilon} H_y \right] \\ \frac{\partial B_z}{\partial t} &= \left[ \frac{\partial E_x}{\partial y} - \frac{\partial E_y}{\partial x} - \frac{\sigma_x}{\epsilon} B_z \right], & \frac{\partial}{\partial t} B_z + \frac{\sigma_z}{\epsilon} B_z &= \mu \left[ \frac{\partial}{\partial t} H_z + \frac{\sigma_y}{\epsilon} H_z \right] \end{aligned}$$

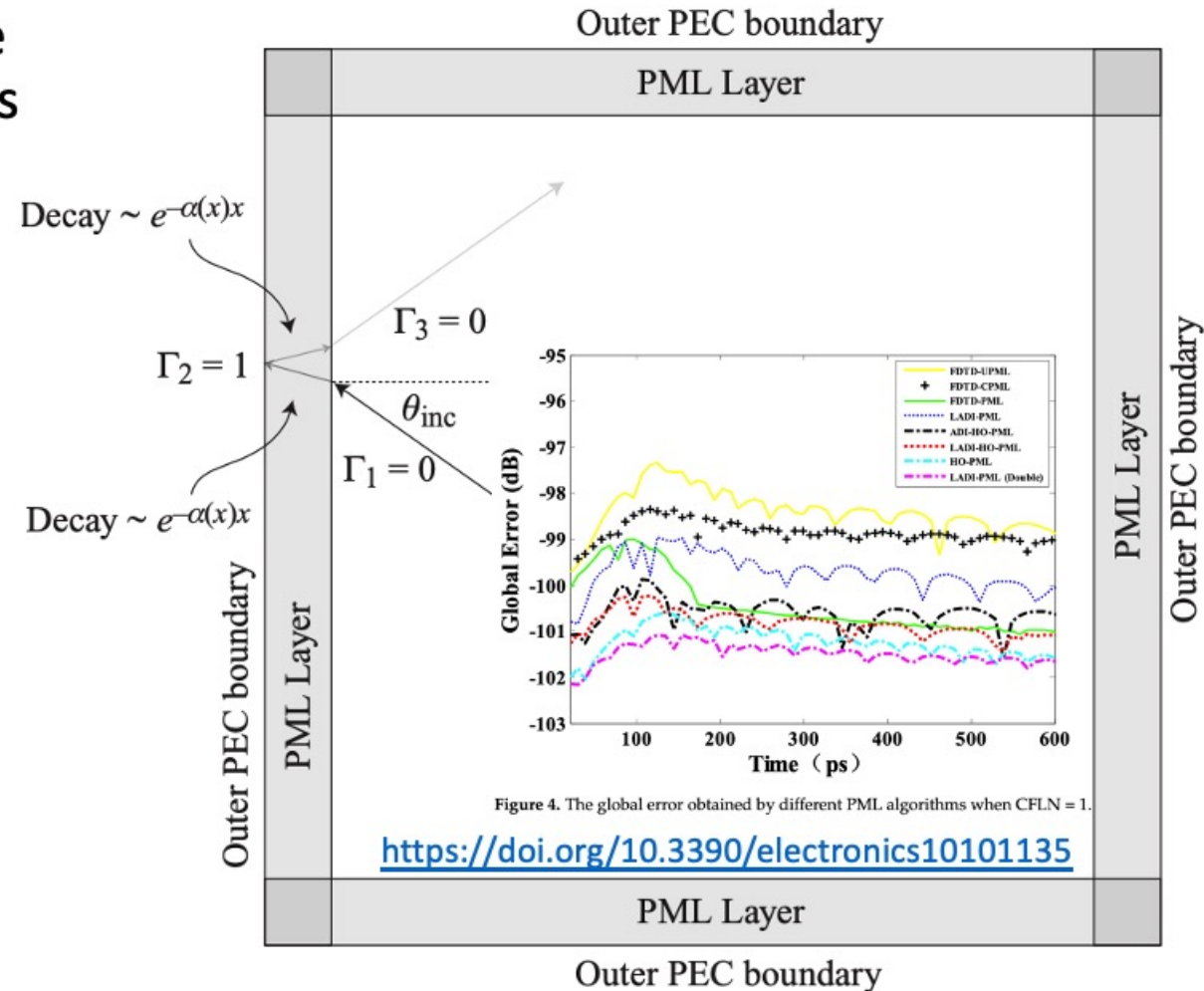
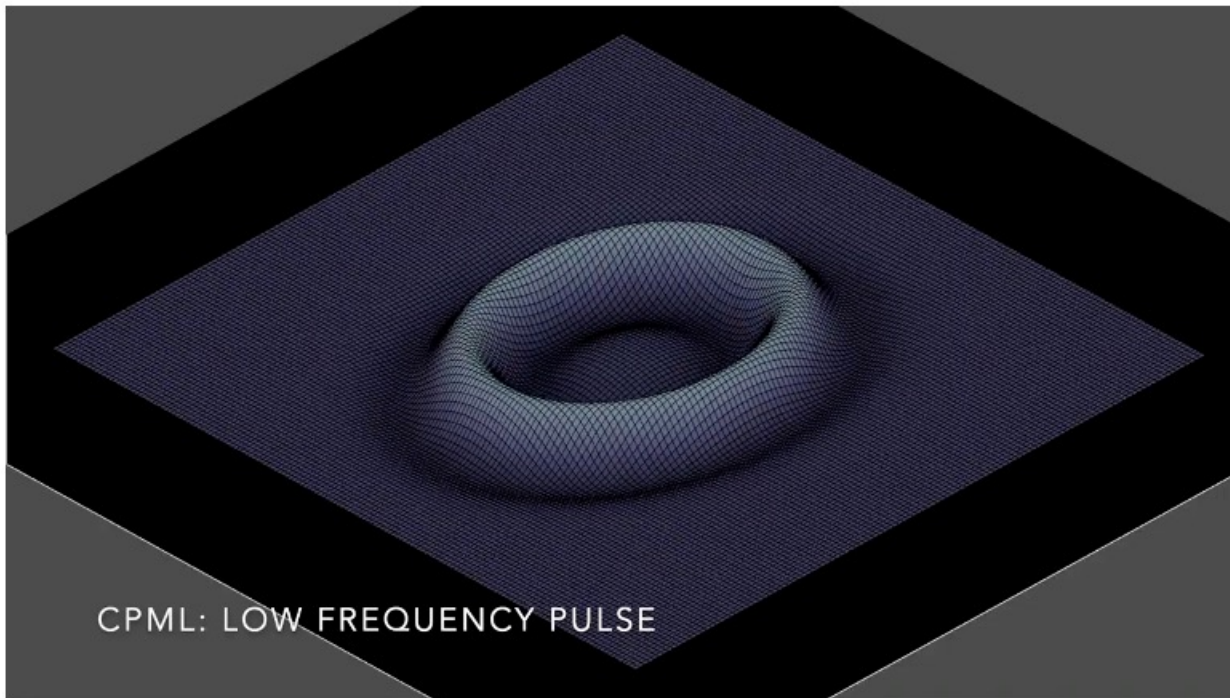


# Particle methods for laser-produced plasmas

## EM fields – FDTD – boundary conditions

Simulation techniques  
in hot plasma modeling

- The efficiency of PML boundary conditions can be tailored via their thickness, and material constants



- **Non-Standard Finite-Difference Time-Domain**  $D_t \mathbf{B} = -\nabla^* \times \mathbf{E}$   
 $D_t \mathbf{E} = \nabla \times \mathbf{B} - \mathbf{J}$

$$\nabla^* = D_x^* \hat{\mathbf{x}} + D_y^* \hat{\mathbf{y}} + D_z^* \hat{\mathbf{z}} \text{ where } D_x^* = (\alpha + \beta S_x^1 + \xi S_x^2) D_x \text{ with } \alpha + 4\beta + 4\xi = 1.$$

$$S_x^1 G_{i,j,k}^n = G_{i,j+1,k}^n + G_{i,j-1,k}^n + G_{i,j,k+1}^n + G_{i,j,k-1}^n,$$

$$S_x^2 G_{i,j,k}^n = G_{i,j+1,k+1}^n + G_{i,j-1,k+1}^n + G_{i,j+1,k-1}^n + G_{i,j-1,k-1}^n$$

- The operators along y and z are obtained by circular permutation of the indices.

Assuming cubic cells ( $\Delta x = \Delta y = \Delta z$ ), the coefficients given in (Karkkainen et al. 2006) ( $\alpha = 7/12$ ,  $\beta = 1/12$  and  $\xi = 1/48$ ) allow for the Courant condition to be at  $\Delta t = \Delta x$ , which equates to having no numerical dispersion along the principal axes. The algorithm reduces to the FDTD algorithm with  $\alpha = 1$  and  $\beta = \xi = 0$ . An extension to non-cubic cells is provided by Cowan,

- **Pseudo Spectral Time Domain** - used to be very popular, before being replaced by finite-difference methods with the advent of parallel supercomputers that favored local methods.

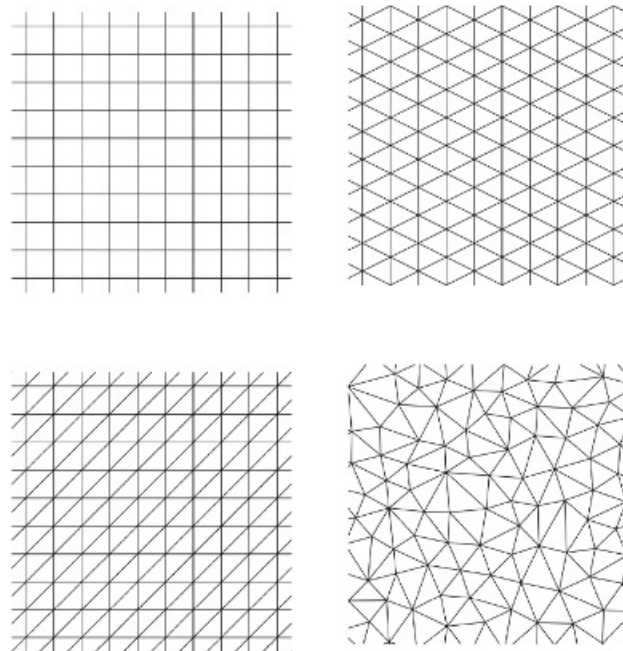


# Particle methods for laser-produced plasmas

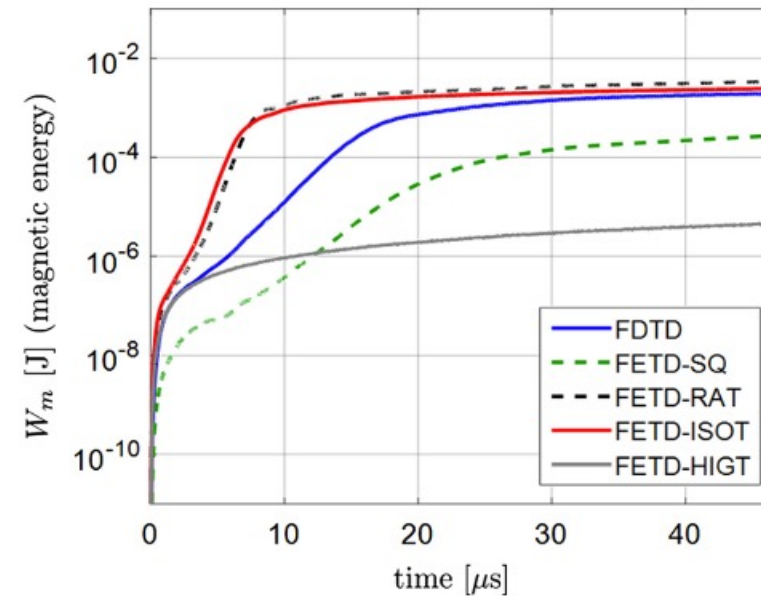
## EM fields – Finite element method

Simulation techniques  
in hot plasma modeling

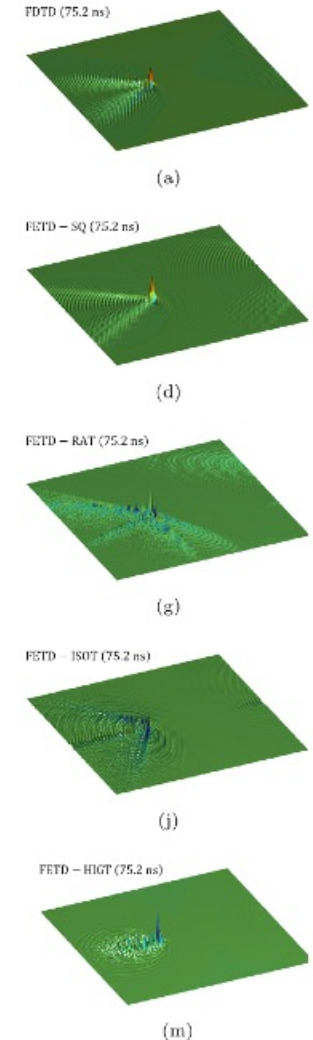
- Finite difference method can be replaced with **finite elements** on an unstructured mesh
- This method is not very common
- Spurious energy produced by numerical Cherenkov radiation on the unstructured mesh reaches saturation levels that are considerably lower than those on meshes based on periodic layout of elements.



Snapshots of the magnetic field distribution resulting from EM-PIC simulations of a single electron-positron pair moving relativistically.



Evolution of the magnetic energy  $W_m$  due to NCR on various meshes.



## Current deposition

- Advantageous to avoid solving the Poisson equation - nonlocal
- Poisson eq. satisfied initially, and continuity eq. respected numerically!!
- Staggered Yee's grid - charge density at the centers of the cells  $\rho_{i+1/2, j+1/2, k+1/2}$
- Particle moves - generates current - straightforward interpolation

$$\mathbf{J} = \sum_n \mathbf{V}_n S_n^\rho \quad S^\rho(\mathbf{x}) = S_x^\rho(x) S_y^\rho(y) S_z^\rho(z)$$

- **Does not work!!** - the continuity equation not satisfied, i.e. the current flux through a cell's boundaries does not represent the actual charge change in the cell (E field not consistent with Poisson)
- Currents can be self-consistent - follow the particle trajectory in detail, and keep recording of how much charge has passed through each of the cell's boundaries
- The current deposition often involves many cells and is computationally demanding
- Different methods – most general applicable to general shape functions – Esirkepov

# Particle methods for laser-produced plasmas

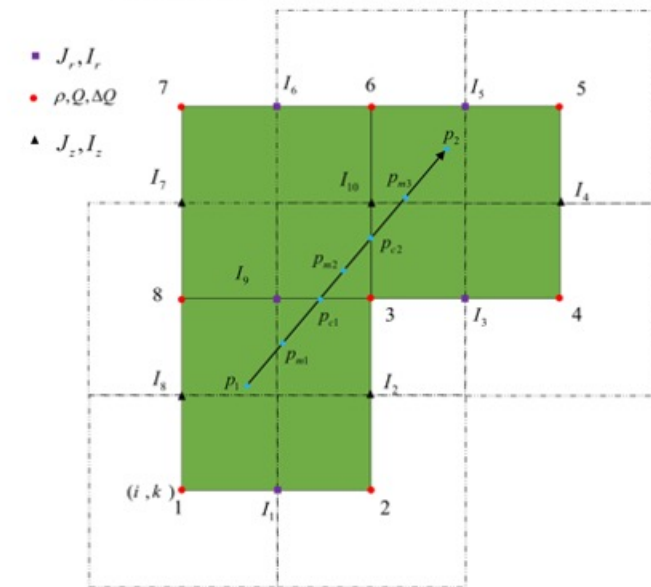
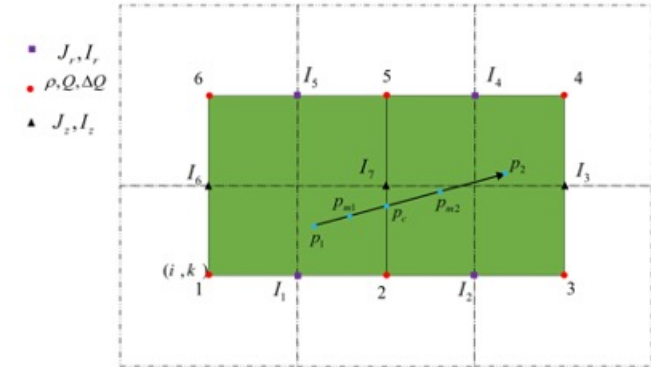
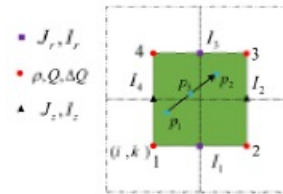
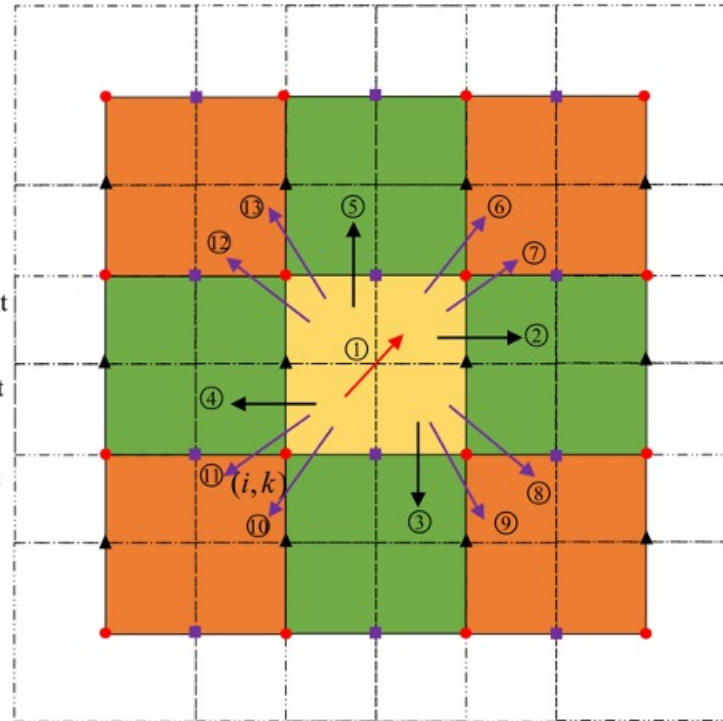
## Current deposition

## Simulation techniques in hot plasma modeling

- Example <https://doi.org/10.1016/j.cpc.2021.107893>
- particle movement in one cell, such as 1
- particle movement in two cells, such as 2-5
- particle movement in three cells, such as 6-14

- $J_r, I_r$
- $\rho, Q$
- ▲  $J_z, I_z$

- ↑ Particle movement in one cell
- ↕ Particle movement in two cells
- ↗ Particle movement in three cells





# Particle methods for laser-produced plasmas

Simulation techniques  
in hot plasma modeling

## Equation of motion – relativity

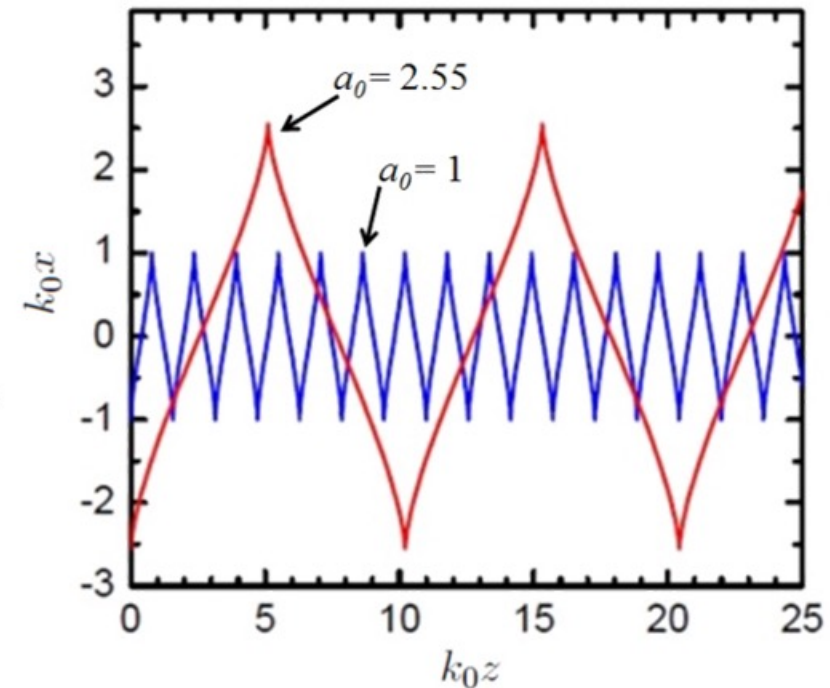
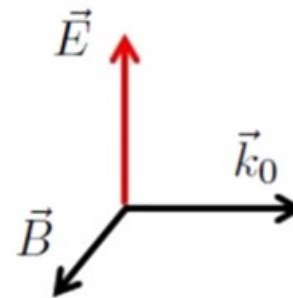
- Where the dynamics starts to be relativistic?  $\frac{d\mathbf{p}}{dt} = -e\mathbf{E} = e\frac{\partial\mathbf{A}}{\partial t}$   $\mathbf{A}(z) = A_0 \sin(k_0z - \omega_0t)\mathbf{e}_x$

$$a_0 = eE_L/(mc\omega_0) \quad a_0 = \sqrt{\frac{e^2}{2\pi^2\epsilon_0 m_e^2 c^5} \lambda_0^2 I_0} \simeq 0.86 \lambda_0 [\mu\text{m}] \sqrt{I_0 [10^{18} \text{ W/cm}^2]}$$

- Solving the equation of motion

$$\beta = v/c = -\frac{eA_0}{mc} \sin(\omega_0t) \triangleq -a_0 \sin(\omega_0t)$$

- $a_0 \ll 1$  non-relativistic
- $a_0 \gtrsim 1$  fully relativistic



## Equation of motion – particle pusher

- In the relativistic case, we need to solve  $\frac{d(m\mathbf{v})}{dt} = q(\mathbf{E} + \mathbf{v} \times \mathbf{B})$   $m = \gamma m_0$

- In PIC method, we often use normalized momentum  $\mathbf{u} = \gamma \mathbf{v}$ .  $\gamma = \frac{1}{\sqrt{1 - (\frac{v}{c})^2}}$

$$\mathbf{u} = \frac{c}{\sqrt{c^2 - |\mathbf{v}|^2}} \mathbf{v} \quad \gamma_u = \sqrt{1 + |\mathbf{u}|^2/c^2}$$

- The eq. of motion is thus solved in the form  $\frac{d\mathbf{u}}{dt} = \frac{q}{m_0} \left( \mathbf{E} + \frac{c}{\sqrt{c^2 + |\mathbf{u}|^2}} \mathbf{u} \times \mathbf{B} \right)$

- To calculate new position, we need to know velocity to

$$\mathbf{x}^{n+1/2} = \mathbf{x}^n + \frac{\mathbf{u}^n}{2\gamma^n} \Delta t,$$

$$\mathbf{v} = \mathbf{u}/\gamma_u = \frac{c}{\sqrt{c^2 + u_x^2 + u_y^2 + u_z^2}} \mathbf{u}$$

$$\frac{\mathbf{u}^{n+1} - \mathbf{u}^n}{\Delta t} = \frac{q}{m} (\mathbf{E}(\mathbf{x}^{n+1/2}) + \bar{\mathbf{v}} \times \mathbf{B}(\mathbf{x}^{n+1/2})),$$

$$\mathbf{x}^{n+1} = \mathbf{x}^{n+1/2} + \frac{\mathbf{u}^{n+1}}{2\gamma^{n+1}} \Delta t.$$

# Particle methods for laser-produced plasmas

## Equation of motion – particle pusher

- Different pushers

- Boris

$$\bar{\mathbf{v}} = \frac{\mathbf{u}^{n+1} + \mathbf{u}^n}{2\gamma^{n+1/2}}$$

- Vay

$$\bar{\mathbf{v}} = \frac{\mathbf{u}^n/\gamma^n + \mathbf{u}^{n+1}/\gamma^{n+1}}{2}$$

- HC

$$\bar{\mathbf{v}} = \frac{\mathbf{u}^{n+1} + \mathbf{u}^n}{2\bar{\gamma}} \quad \bar{\gamma} = \sqrt{1 + \left(\frac{\mathbf{u}^{n+1} + \mathbf{u}^n}{2c}\right)^2}$$

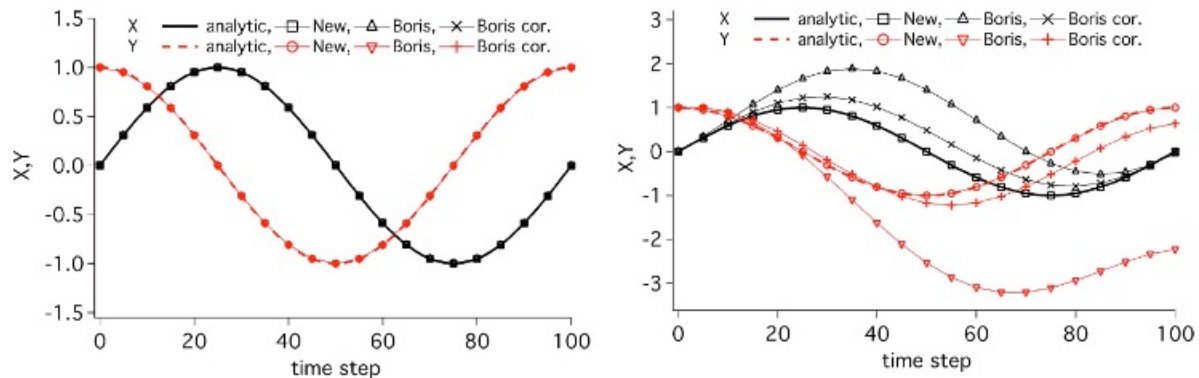


FIG. 1. (Color online) X and Y positions vs time step of a particle rotating in a constant magnetic field  $B_z$  as computed in the laboratory (left) or in a frame moving along  $\hat{y}$  at  $\gamma=2$  (right).

<https://doi.org/10.1063/1.2837054>

## Simulation techniques in hot plasma modeling

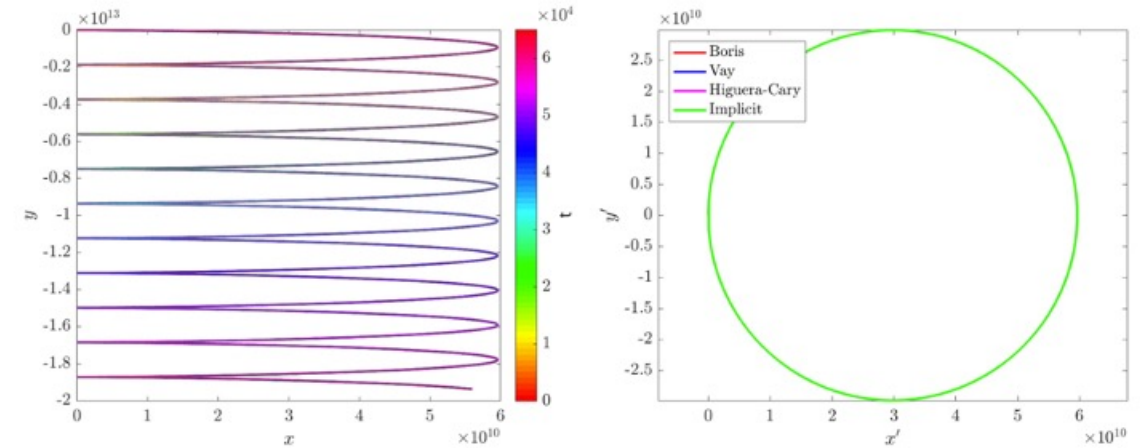


Figure 6. Trajectory of the particle colored by time in the observer frame (left-hand panel) and colored by method in the comoving  $E \times B$  frame (right-hand panel) for  $\kappa = 10$ .

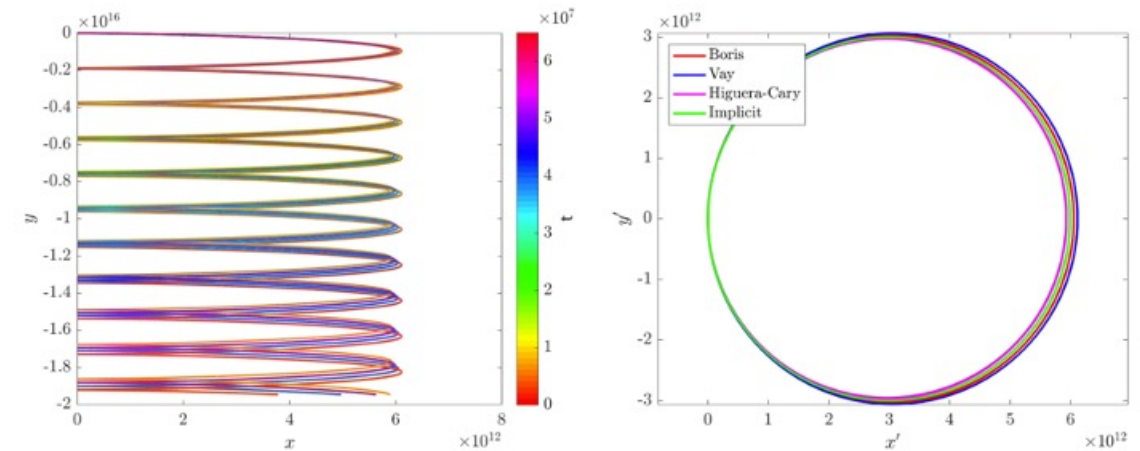


Figure 7. Trajectory of the particle colored by time in the observer frame (left-hand panel) and colored by method in the comoving  $E \times B$  frame (right-hand panel) for  $\kappa = 100$ .

<https://doi.org/10.3847/1538-4365/aab114>



## EM fields – Envelope approximation

- In many situations, the spatial and temporal scales of interest (related to e.g. plasma waves) are much larger than laser wavelength/period
- One only needs to sample the laser envelope (slowly varying)  $\tilde{\mathbf{A}}$

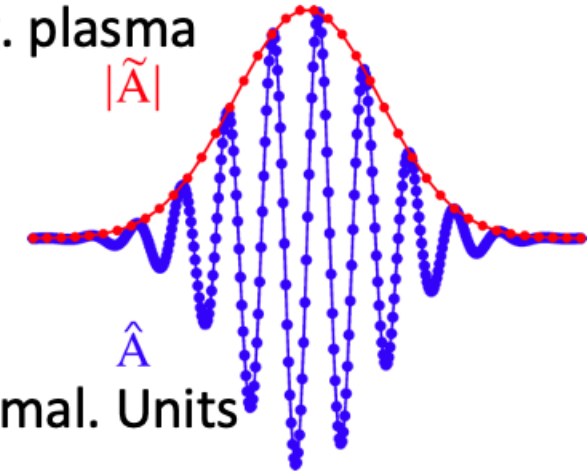
$$\hat{\mathbf{A}}(\mathbf{x}, t) = \text{Re} \left[ \tilde{\mathbf{A}}(\mathbf{x}, t) e^{ik_0(x-ct)} \right]$$

- The evolution of the laser pulse is described by d'Alembert's equation in normal. Units  $\nabla^2 \hat{\mathbf{A}} - \partial_t^2 \hat{\mathbf{A}} = -\hat{\mathbf{J}}$  (fast oscillating current)
- Can be reduced to envelope equation  $\nabla^2 \tilde{\mathbf{A}} + 2i \left( \partial_x \tilde{\mathbf{A}} + \partial_t \tilde{\mathbf{A}} \right) - \partial_t^2 \tilde{\mathbf{A}} = \chi \tilde{\mathbf{A}}$

with the plasma susceptibility  $\chi(\mathbf{x}) = \sum_s \frac{q_s^2}{m_s} \sum_p \frac{w_p}{\bar{\gamma}_p} S(\mathbf{x} - \bar{\mathbf{x}}_p)$  containing average Lorentz factor of macroparticle

- The equation of motion is given by averaged EM fields with the addition of the ponderomotive force

$$\mathbf{F}_{pond} = -r_s^2 \frac{1}{4\bar{\gamma}_p} \nabla \left( |\tilde{\mathbf{A}}|^2 \right) \quad r_s = q_s/m_s$$



- The equation of motion is thus

$$\frac{d\bar{\mathbf{u}}_p}{dt} = r_s \left( \bar{\mathbf{E}}_p + \frac{\bar{\mathbf{u}}_p}{\bar{\gamma}_p} \times \bar{\mathbf{B}}_p \right) - r_s^2 \frac{1}{4\bar{\gamma}_p} \nabla \left( |\tilde{\mathbf{A}}_p|^2 \right)$$

- Maxwell's equations remain unaltered, but do not contain the laser field

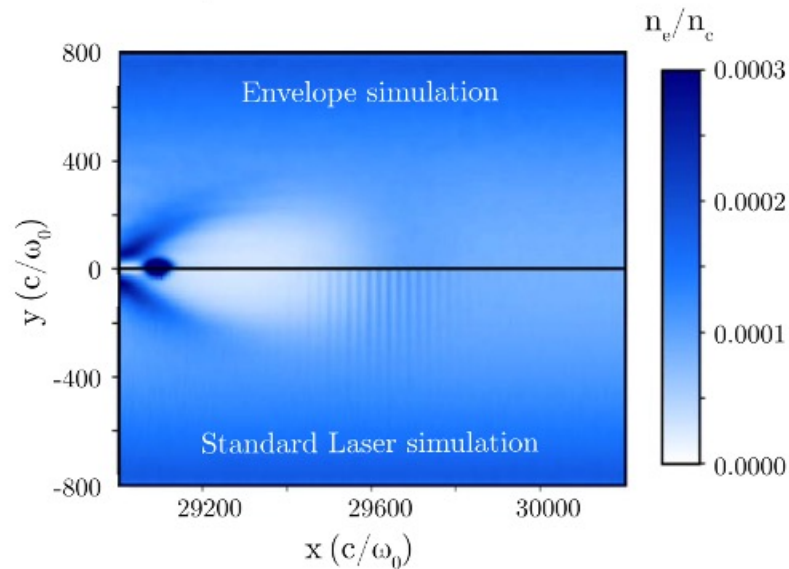


**Figure 4.** Plasma density after 3.7 mm of propagation. Top panel: results obtained with the envelope model. Bottom panel: results obtained through a standard laser simulation.

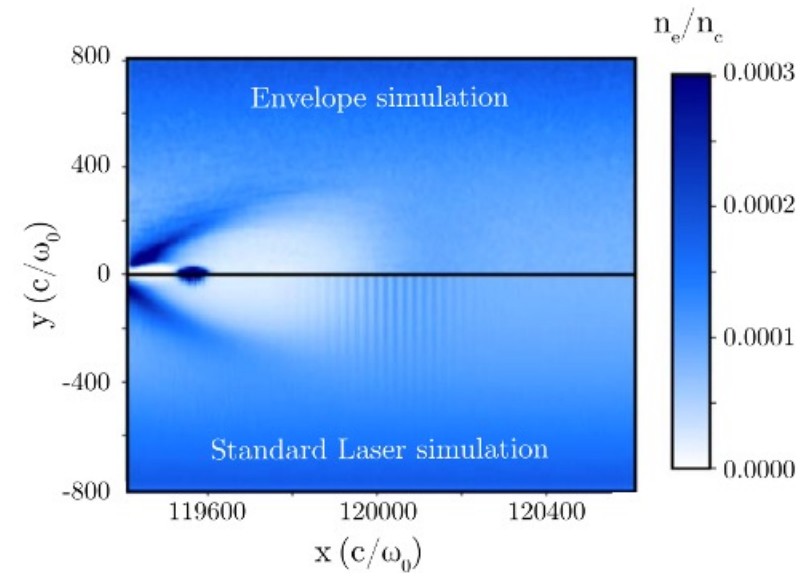


**Figure 6.** Plasma density after 15 mm of propagation. Top panel: results obtained with the envelope model. Bottom panel: results obtained through a standard laser simulation.

# Particle methods for laser-produced plasmas

## Advanced techniques – Moving frame

Simulation techniques  
in hot plasma modeling

- Simulations of plasma accelerators from first principles are extremely computationally intensive - need to resolve the evolution of a driver
- Moving window used to follow the driver
  - significant speedup

<https://doi.org/10.1088/0741-3335/58/3/034018>

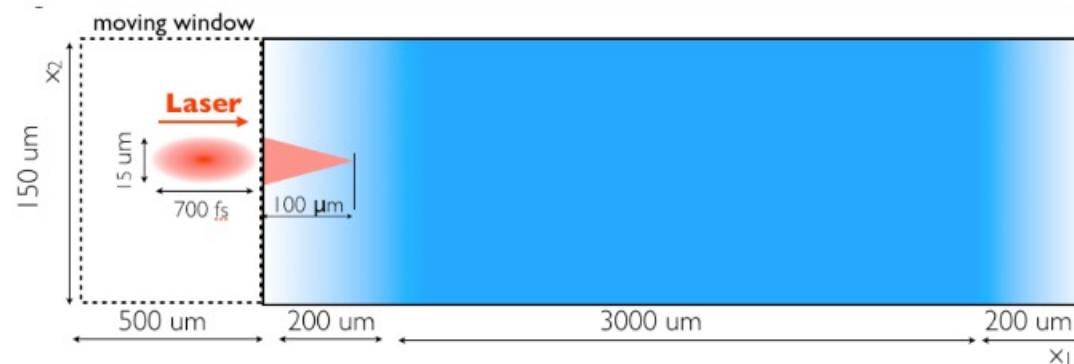
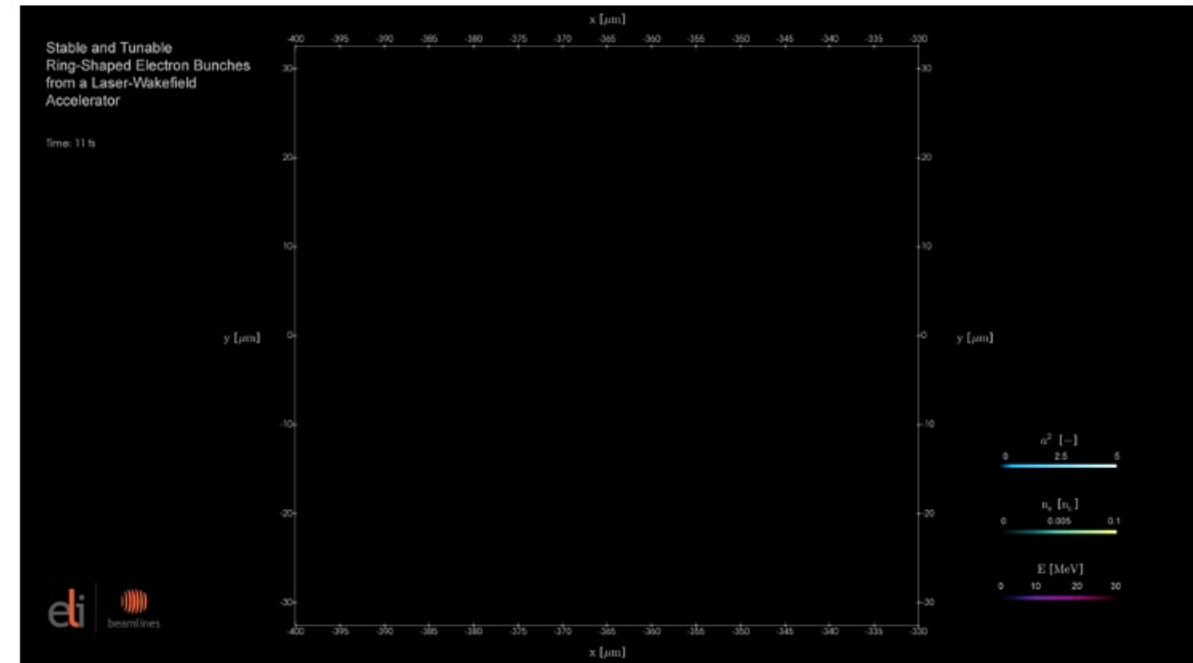
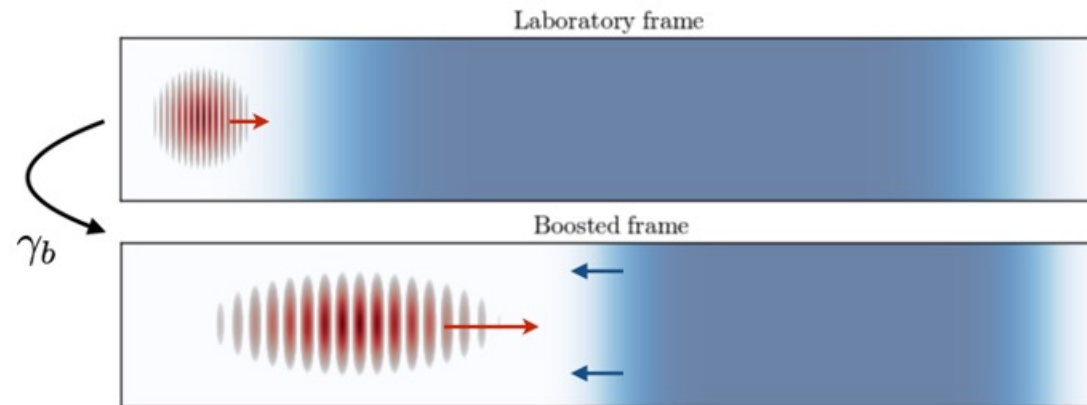


Figure 1 - Layout of the 2D PIC simulation in the speed-of-light frame with a box that was 500 x 150 μm with 30000 x 1024 cells. The laser had an  $a_0 = 1.5$  or 3 and was focused 100 μm into the 200-μm-long density up-ramp in a region of fully-ionized He plasma. The density ramp was followed by a 3000 μm constant density region and end with a 200-μm-long-density down ramp.





- Full PIC simulation of a plasma accelerator very demanding even with moving window
- Choosing an optimal frame of reference that travels close to the speed of light in the direction of the laser beam enables speedups by orders of magnitude



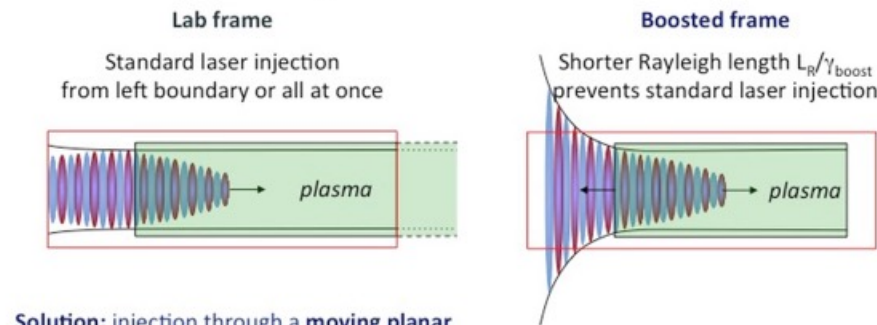
- In a frame moving with the driver beam in the plasma at velocity  $v = \beta c$  the beam length is increased by  $\approx (1 + \beta)\gamma$  while the plasma contracts by  $\gamma$
- Converting input parameters from the lab frame to the boosted frame
- Converting results to the lab frame (non-simultaneity between Lorentz frames)

# Particle methods for laser-produced plasmas

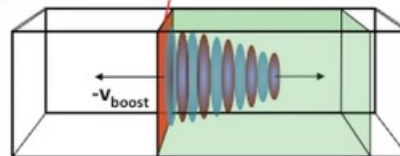
## Advanced techniques – Lorentz boost frame

Simulation techniques  
in hot plasma modeling

- Modified scales  $\lambda'_0 = \gamma(1 + \beta)\lambda_0$   $a'_0 = a_0/\gamma(1 + \beta)$   
 $L'_{\text{pulse}} = \gamma(1 + \beta)L_{\text{pulse}}$   $L'_{\text{plasma}} = L_{\text{plasma}}/\gamma$   
 $L'_{\text{pulse}}/L'_{\text{plasma}} = \gamma^2(1 + \beta)L_{\text{pulse}}/L_{\text{plasma}}$
- Non-simultaneity between Lorentz frames do not allow for a direct comparison between boosted frame and laboratory frame
- Temporal snapshot in the laboratory frame several boosted frame snapshots are required
- Initialization may be difficult but can be solved with antenna



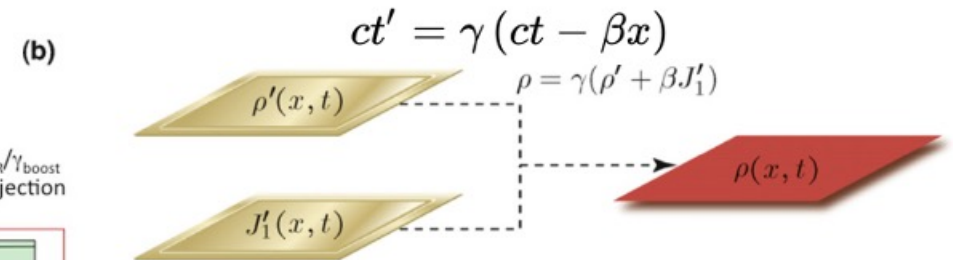
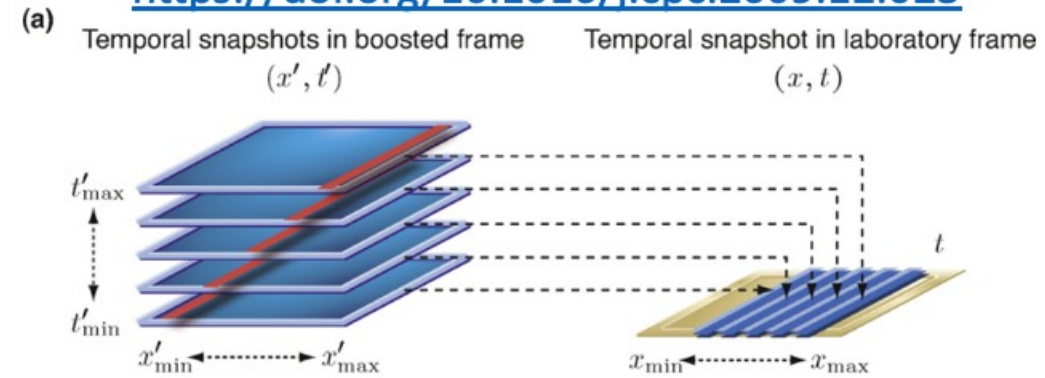
Solution: injection through a moving planar antenna in front of plasma\*



• Laser injected using macroparticles using Esirkepov current deposition ==> verifies Gauss' Law.

• For high  $\gamma_{\text{boost}}$  backward radiation is blue shifted and unresolved.

<https://doi.org/10.1016/j.cpc.2009.12.023>



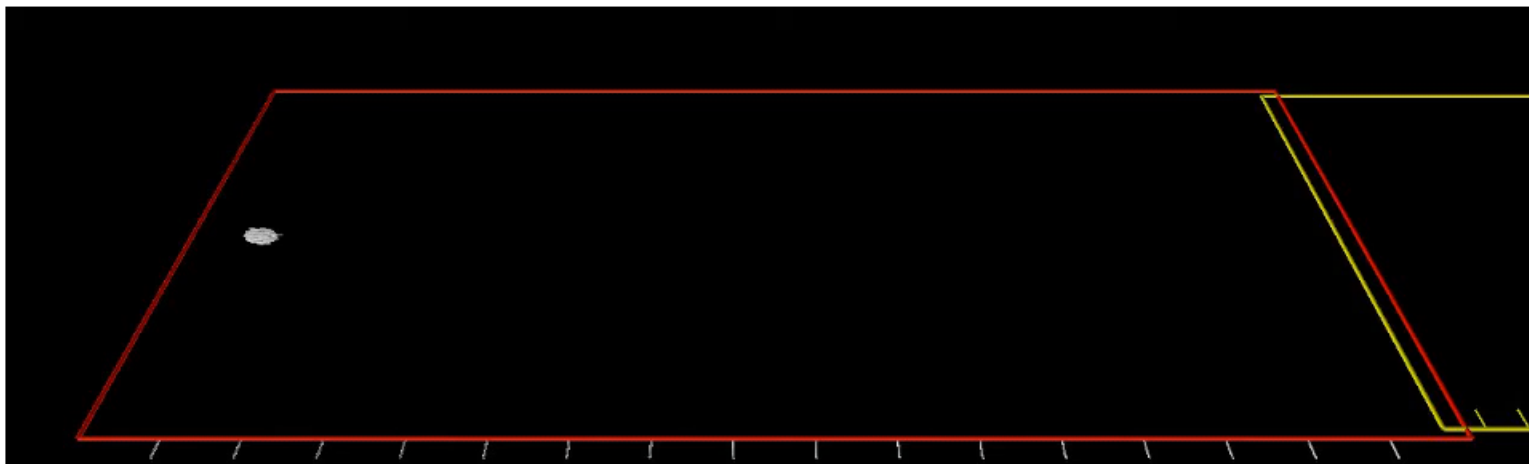
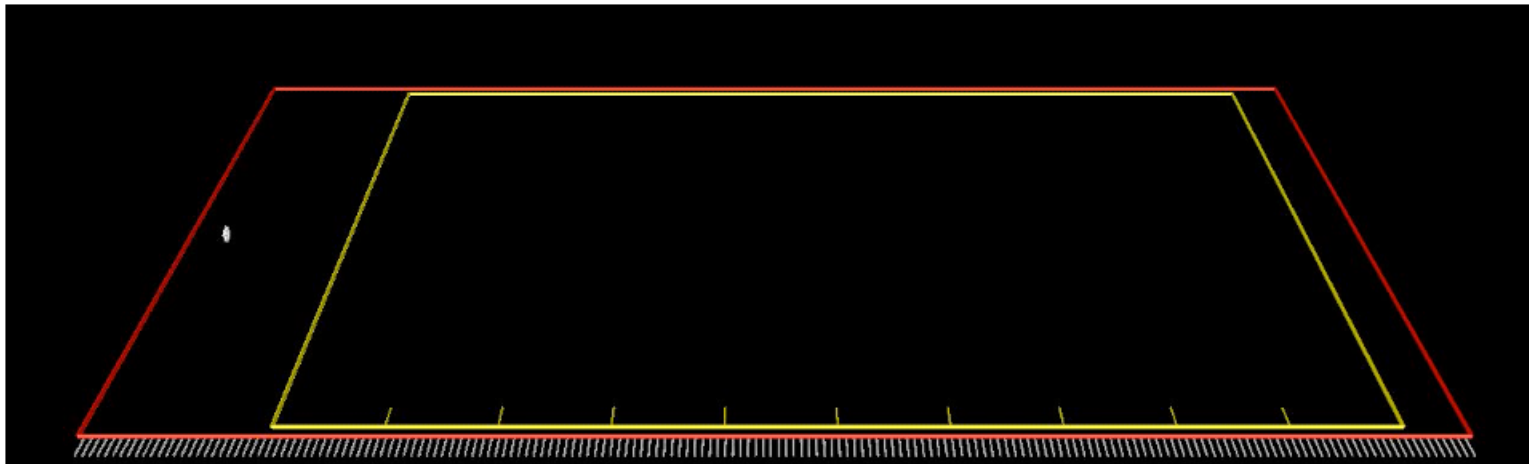
# Particle methods for laser-produced plasmas

## Advanced techniques – Lorentz boost frame

Simulation techniques  
in hot plasma modeling

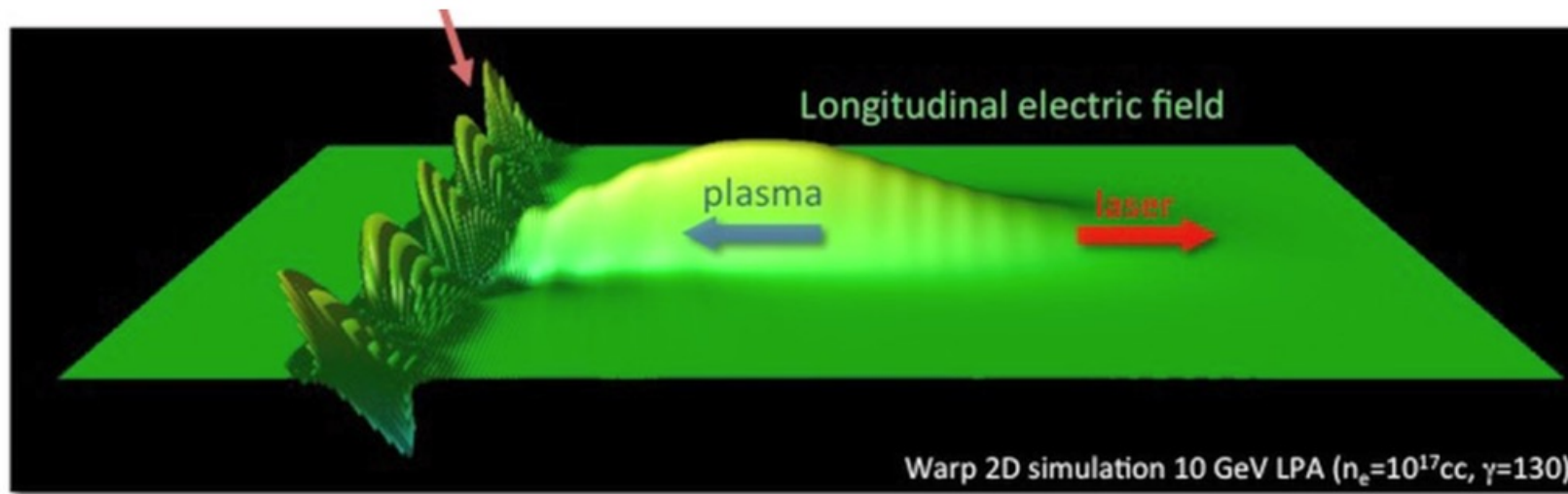
<https://www.youtube.com/watch?v=gG2KlgfdS2Q>

[https://www.youtube.com/watch?v=r\\_qJxT2Co2w](https://www.youtube.com/watch?v=r_qJxT2Co2w)





<https://vimeo.com/235349519>



Is it numerical Cherenkov instability?

BTW, what is “numerical Cherenkov instability”?

# Particle methods for laser-produced plasmas

## Advanced techniques – Numerical Cherenkov

Simulation techniques  
in hot plasma modeling

- **Numerical Cherenkov radiation (NCR) instability** - important detrimental factor in EM-PIC simulations involving relativistic charged particles
- Associated with regular periodic meshes such as used by FDTD method & numerical velocity of electromagnetic waves in vacuum is lower than the speed of light (slow down of poorly-resolved waves)

<https://www.youtube.com/watch?v=VNftf5qLpiA>

- aliasing mechanisms
- numerical dispersion

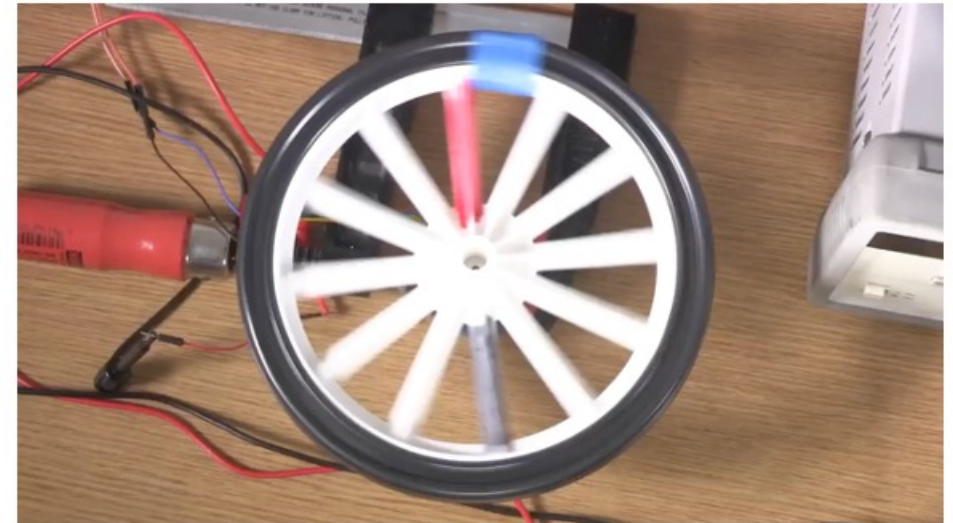
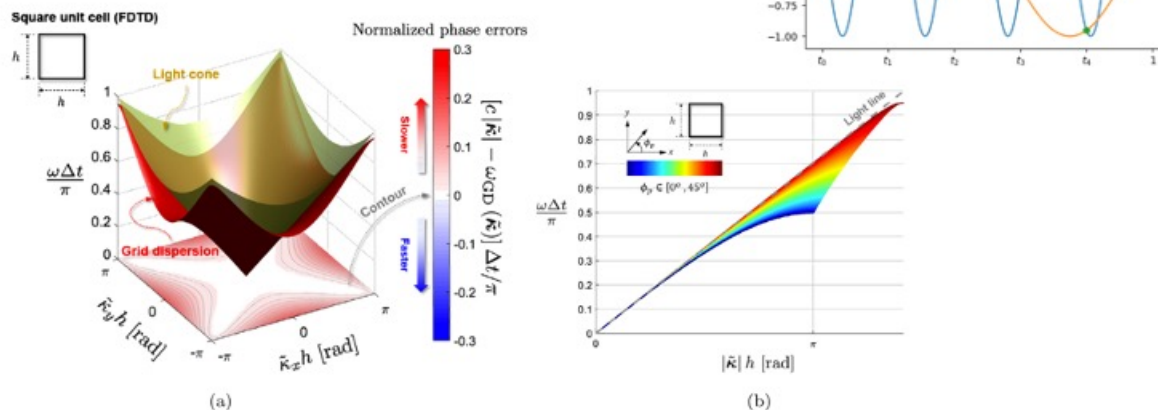


Fig. 1. Numerical grid dispersion of the 2-D Yee's FDTD scheme on a structured mesh. (a) The red color surface represents the dispersion diagram of the normalized frequency  $\omega \Delta t / \pi$  versus the normalized numerical wavenumber  $\tilde{\mathbf{k}} h$  in radians. The olive color surface represents the light cone. The contour levels at the bottom represent the normalized phase errors (with respect to the color bar). (b) Wavenumber magnitude versus frequency for different wave propagation angles with respect to the x axis,  $\phi_p \in [0^\circ, 45^\circ]$ .  
this article.)

<https://doi.org/10.1016/j.jcp.2019.108880>



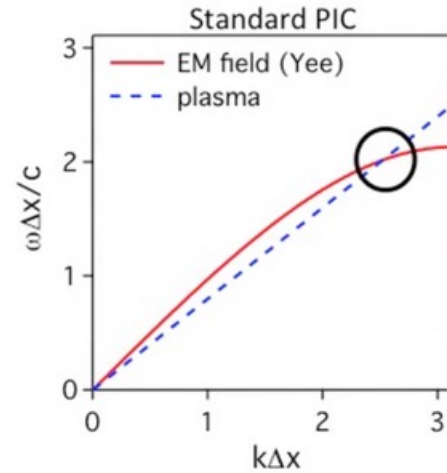
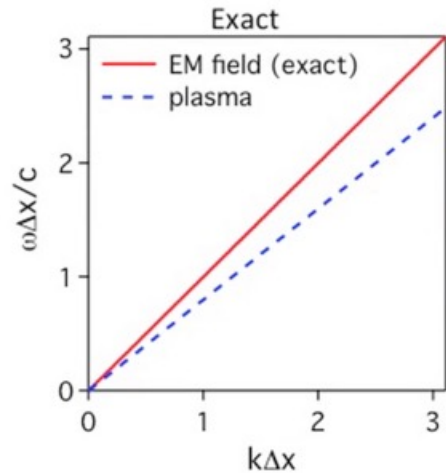
# Particle methods for laser-produced plasmas

## Advanced techniques – Numerical Cherenkov

Simulation techniques  
in hot plasma modeling

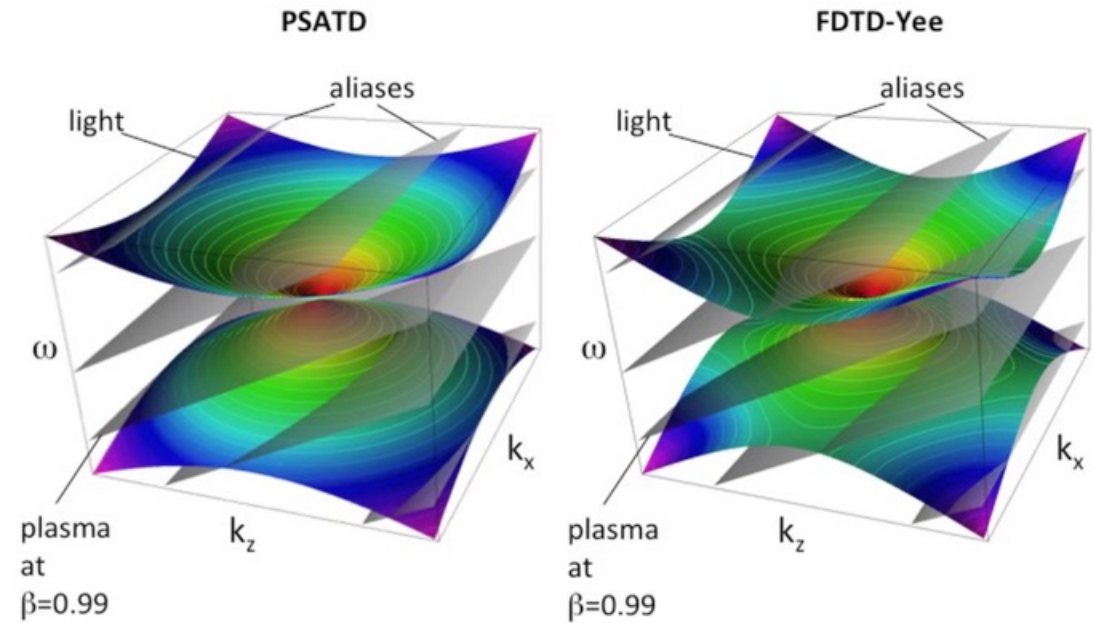
<https://vimeo.com/235349519>

Lagrangian plasma streaming through Eulerian grid at relativistic velocity



Numerical dispersion leads to crossing of EM field and plasma modes -> instability.

\*B. B. Godfrey, "Numerical Cherenkov instabilities in electromagnetic particle codes", *J. Comput. Phys.* **15** (1974)



Need to consider at least first aliases  $m_x = \{-3...+3\}$  to study stability.



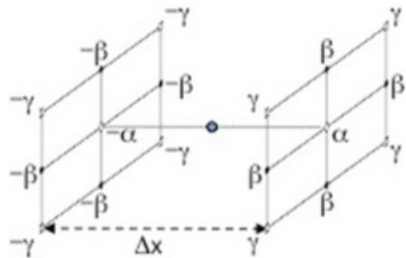
# Particle methods for laser-produced plasmas

## Advanced techniques – Numerical Cherenkov

Simulation techniques  
in hot plasma modeling

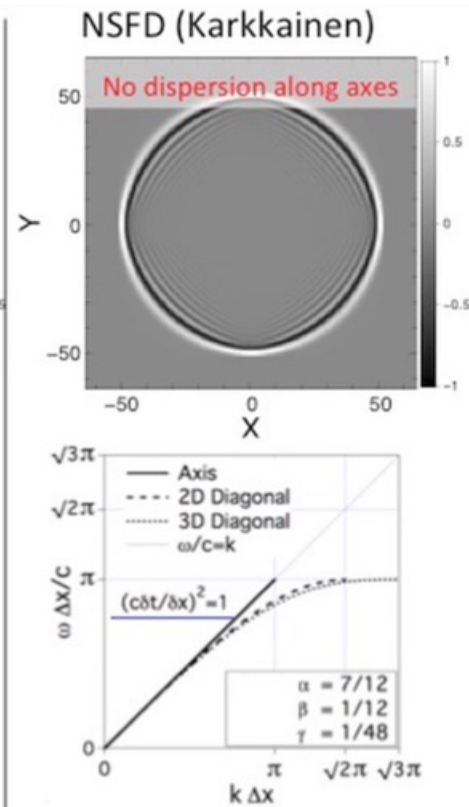
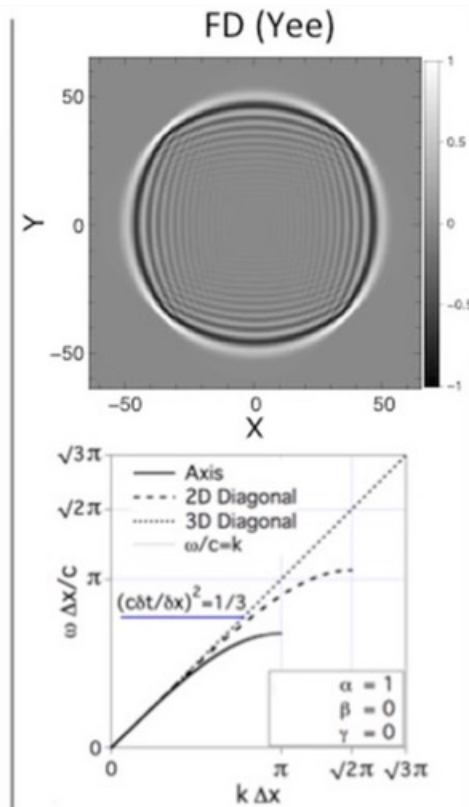
<https://vimeo.com/235349519>

NSFD<sup>1,2</sup>: weighted average of quantities transverse to FD ( $\alpha+4\beta+4\gamma=1$ ).



NSFD=FD if  $\alpha=1, \beta=\gamma=0$ .

Pukhov algo<sup>3</sup> for 1 set of  $\alpha, \beta, \gamma$



| Pseudo-Spectral Time Domain<br>UPIC-EMMA (UCLA)   | Pseudo-Spectral Analytic<br>Time Domain <sup>1,2</sup><br>Warp (LBNL/LLNL/U. Maryland)  |
|---|---|
|   |   |
| <ul style="list-style-type: none"> <li>Numerical dispersion,</li> <li>isotropy,</li> <li>Courant condition:</li> </ul> $c\Delta t \leq 2/\pi \sqrt{\frac{1}{\Delta x^2} + \frac{1}{\Delta y^2} + \frac{1}{\Delta z^2}}$ | <ul style="list-style-type: none"> <li>Exact dispersion,</li> <li>isotropy,</li> <li>Courant condition:</li> </ul> <p style="text-align: center;"><b>None</b></p> |

<sup>1</sup>J. B. Cole, IEEE Trans. Microw. Theory Tech. **45** (1997).  
J. B. Cole, IEEE Trans. Antennas Prop. **50** (2002).

<sup>2</sup>M. Karkkainen et al., Proc. ICAP, Chamonix, France (2006).  
<sup>3</sup>A. Pukhov, J. Plasma Physics **61** (1999) 425

# Particle methods for laser-produced plasmas

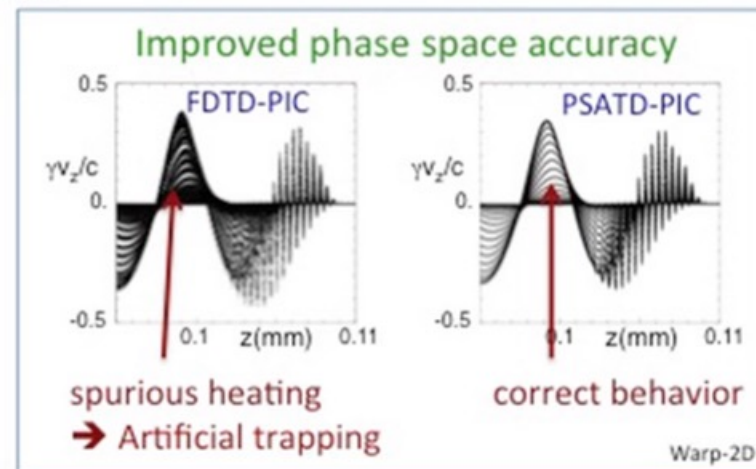
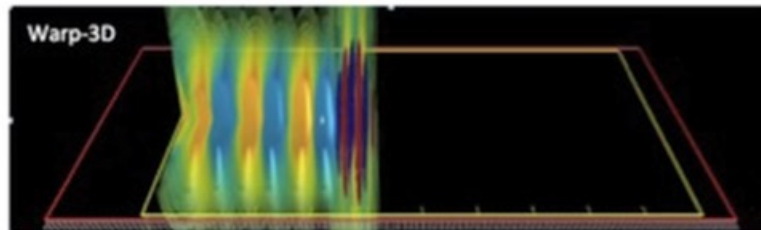
## Advanced techniques – Numerical Cherenkov

Simulation techniques  
in hot plasma modeling

<https://vimeo.com/235349519>

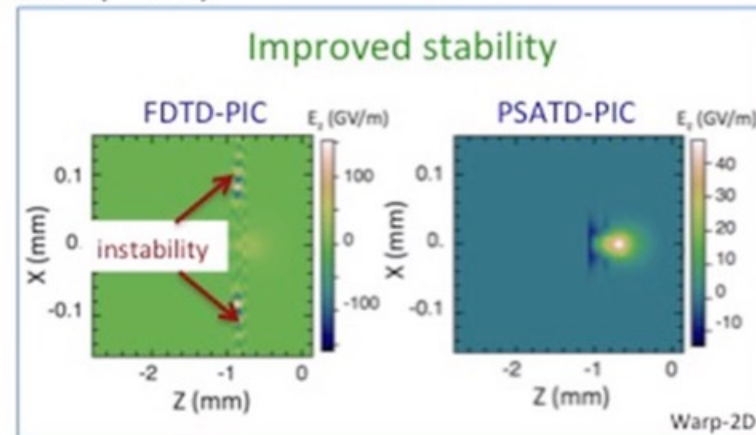
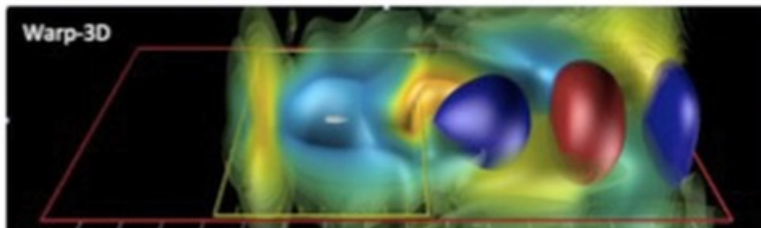
Lab frame

Short laser propagates into long plasma channel,  
electron beam accelerated in wake.



Lorentz boosted frame (wake)

Modeling in a boosted frame reduces # time steps.  
Plasma drifting near C leads to Num. Cherenkov.



## Field ionization – atomic units

- The natural reference point - hydrogen atom. We can derive many quantities from Bohr's model, with which we can then compare the laser field during interaction

$$a_B = \frac{\hbar^2}{me^2} = 5.3 \times 10^{-9} \text{ cm},$$

- First of all, the Bohr's radius is and the electric field at this distance from the proton in the hydrogen atom is

$$E_a = \frac{e}{4\pi\epsilon_0 a_B^2} \\ \simeq 5.1 \times 10^9 \text{ Vm}^{-1}$$

- So-called atomic intensity - the intensity at which the field of the laser pulse is equal to the field that binds the electron in the hydrogen atom

$$I_a = \frac{\epsilon_0 c E_a^2}{2} \\ \simeq 3.51 \times 10^{16} \text{ Wcm}^{-2}$$

- The laser intensity  $I_L > I_a$  will guarantee the ionization of any target material.

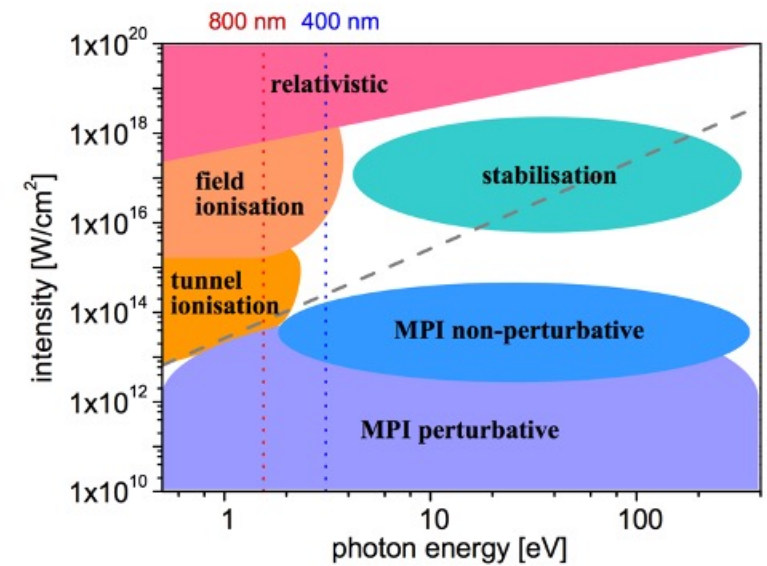
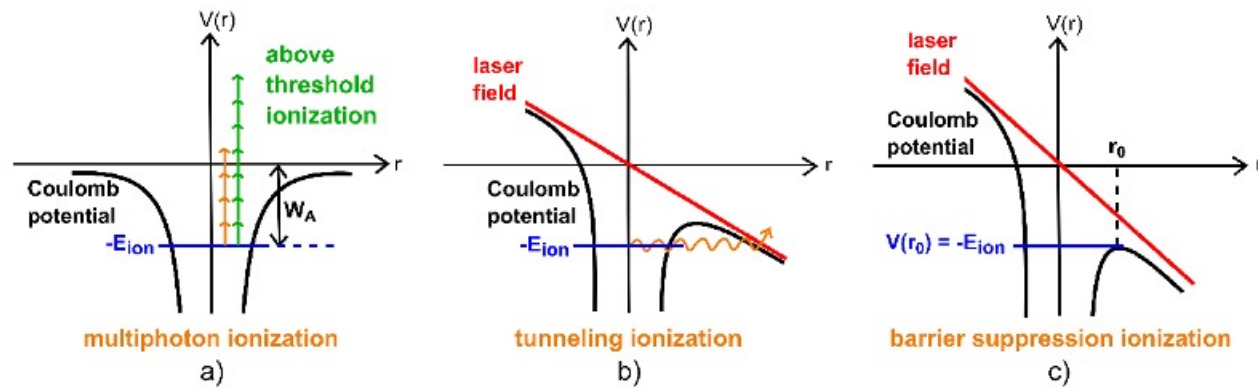


# Particle methods for laser-produced plasmas

## Field ionization – ionization models

Simulation techniques  
in hot plasma modeling

- Ionization often takes place at much lower intensities due to multi-photon absorption.



- Keldysh parameter  $\gamma = \sqrt{\frac{E_I}{2U_P}} = \sqrt{\frac{\epsilon_0 m_e c E_I \omega^2}{q^2 I}}$

- Barrier suppression ionization – appearance intensity

$$I_{\text{app}} \simeq 4 \times 10^9 \left( \frac{E_{\text{ion}}}{\text{eV}} \right)^4 Z^{-2} \text{ Wcm}^{-2}$$

## Field ionization – ionization models

- Tunneling ionization from the ground state of a Hydrogen atom in an electrostatic (DC) field - Landau

$$w = 4\omega_a \frac{E_a}{|E|} \exp\left[-\frac{2}{3} \frac{E_a}{|E|}\right] \quad E_a = \frac{m^2 e^5}{(4\pi\epsilon_0)^3 \hbar^4} \quad \omega_a = \frac{me^4}{(4\pi\epsilon_0)^2 \hbar^3}$$

- Multi-electron atoms 
$$W_{\text{ADK}} = A_{n^*,l^*} B_{l,|m|} I_p \left(\frac{2(2I_p)^{3/2}}{|E|}\right)^{2n^*-|m|-1} \exp\left(-\frac{2(2I_p)^{3/2}}{3|E|}\right)$$

where  $I_p$  is the  $Z^* - 1$  ionization potential of the ion,  $n^* = Z^* / \sqrt{2I_p}$  and  $l^* = n^* - 1$  denote the effective principal quantum number and angular momentum, and  $l$  and  $m$  denote the angular momentum and its projection on the laser polarization direction, respectively.  $W_{\text{ADK}}$ ,  $I_p$  and  $E$  are here expressed in atomic units. The coefficients  $A_{n^*,l^*}$  and  $B_{l,|m|}$  are given by:

$$A_{n^*,l^*} = \frac{2^{2n^*}}{n^* \Gamma(n^*+l^*+1) \Gamma(n^*-l^*)},$$

$$B_{l,|m|} = \frac{(2l+1)(l+|m|)!}{2^{|m|} |m|! (l-|m|)!},$$

- MC procedure - Ionisation occurs if  $U_1 < 1 - \exp(-W \Delta t)$   
for a uniform random number  $U_1 \sim [0, 1]$ .
- $$W_{\text{Field}}(E) = \begin{cases} \min(W_{\text{Multi}}(E), W_{\text{ADK}}(E_T)) & : E \leq E_M \\ W_{\text{ADK}}(E) & : E_M < E \leq E_T \\ \min(W_{\text{ADK}}(E), W_{\text{BSI}}(E)) & : E_T < E \leq E_B \\ W_{\text{BSI}}(E) & : E > E_B \end{cases}$$

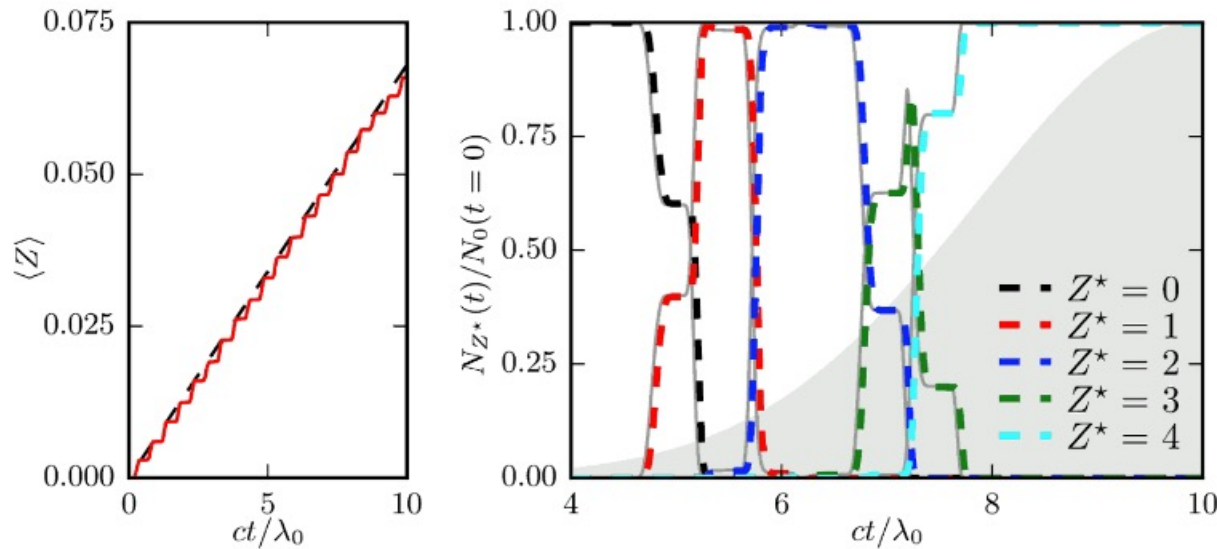
# Particle methods for laser-produced plasmas

## Field ionization – ionization models

Simulation techniques  
in hot plasma modeling

- Ionization current introduced – energy loss

$$\mathbf{J}_{\text{ion}} \cdot \mathbf{E} = \Delta t^{-1} \sum_{j=1}^k I_p (Z^* - 1 + k)$$



<https://www.youtube.com/watch?v=lf3mWR> GYSs

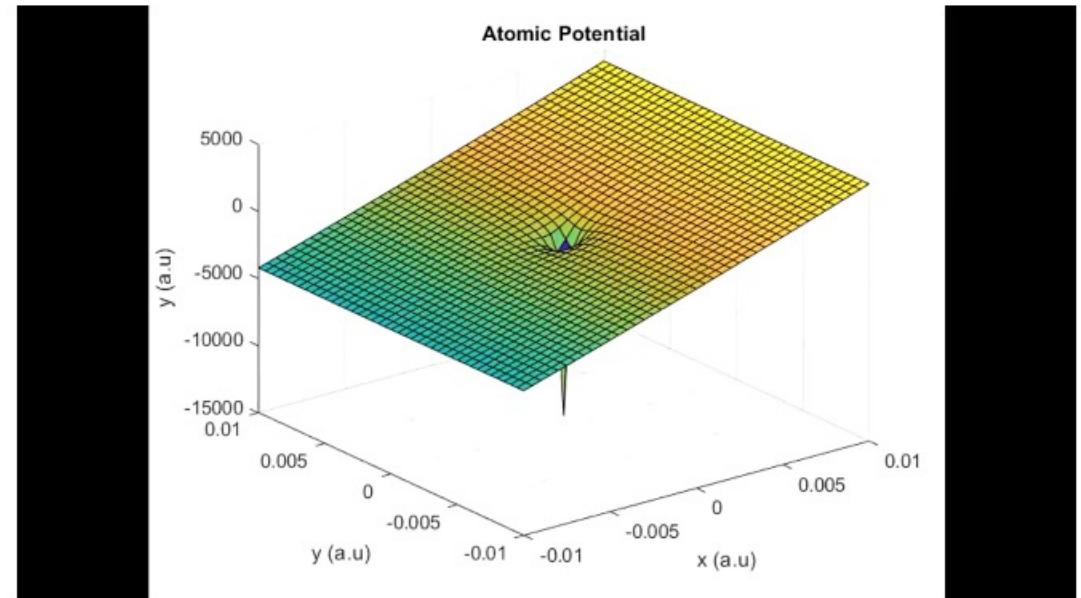


*Fig. 26* | Results of two benchmarks for the field ionization Model. Top: Average charge state of hydrogen ions as a function of time when irradiated by a laser. The red solid line corresponds to PIC results, the dashed line corresponds to theoretical predictions using the cycle-averaged ADK growth rate of (10). Bottom: Relative distribution of carbon ions for different charge states as a function of time. Dashed lines correspond to PIC results, thin gray lines correspond to theoretical predictions obtained from (12). The Gaussian gray shape indicates the laser electric field envelope.

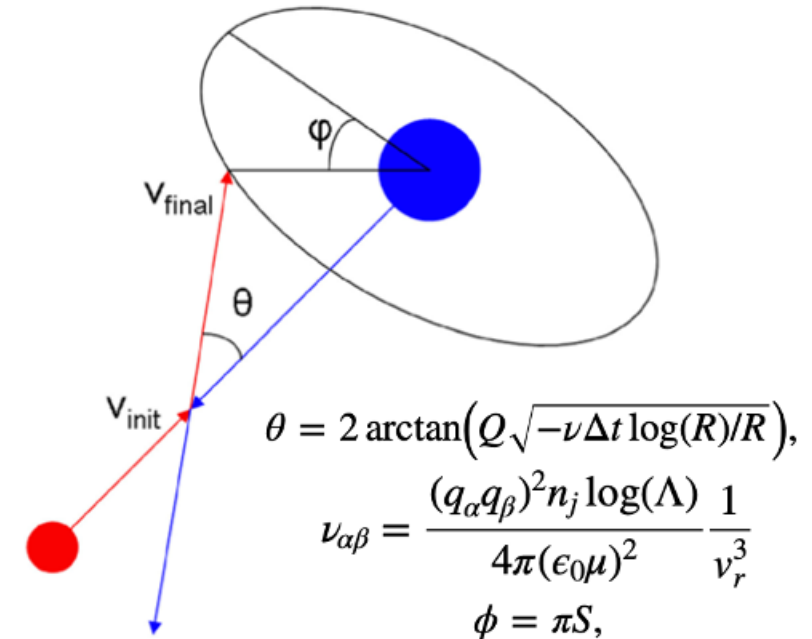
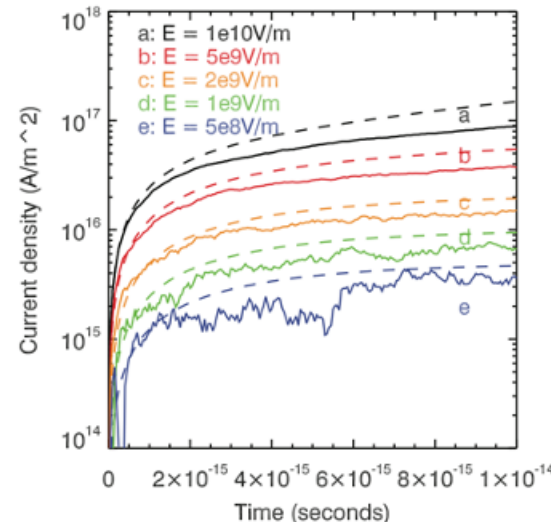


# Particle methods for laser-produced plasmas

## Binary Coulomb collisions

Simulation techniques  
in hot plasma modeling

- Codes generally neglect particle interactions over very short (less than grid scale) ranges.
- At high temperatures ( $\gtrsim 1$  keV) and relatively low densities ( $\lesssim 10^{21}$  cm $^{-3}$ ) collisional effects in plasmas are generally considered minimal.
- Laser produced plasma could however be relatively dense.
- Mostly - binary collision approach - Rutherford scattering on pairs of particles which reside in the same grid cell.
- Collisions calculated in the centre-of-momentum frame of the two particles
- One must also take into account different weights of particles
- Example validation – Spitzer resistivity



$$\theta = 2 \arctan\left(Q \sqrt{-\nu \Delta t \log(R)/R}\right),$$

$$\nu_{\alpha\beta} = \frac{(q_{\alpha}q_{\beta})^2 n_j \log(\Lambda)}{4\pi(\epsilon_0\mu)^2} \frac{1}{v_r^3}$$

$$\phi = \pi S,$$

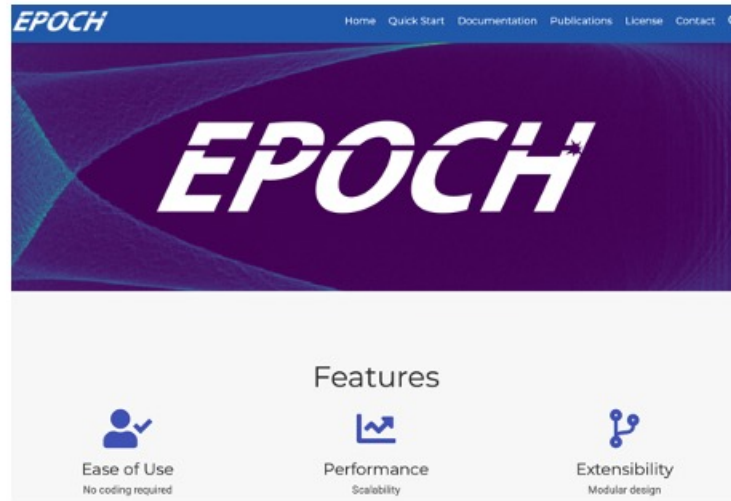
Figure 2. Diagram to illustrate the scattering angles,  $\theta$  and  $\phi$ , that particle  $i$  (red) is scattered through when colliding with particle  $j$  (blue) in the centre-of-momentum frame.

# Particle methods for laser-produced plasmas

## Available PIC codes

- <https://epochpic.github.io>
- <https://smileipic.github.io>
- <https://picongpu.readthedocs.io/>
- <https://warpX.readthedocs.io>

Simulation techniques  
in hot plasma modeling

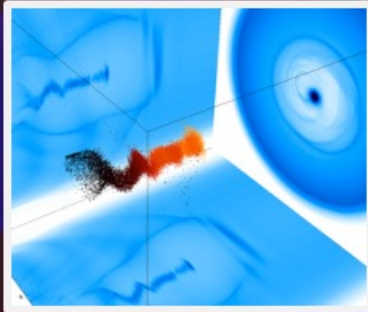




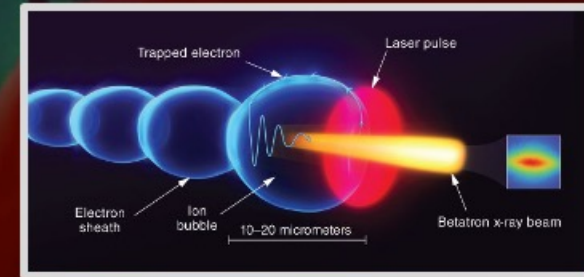
# Particle methods for laser-produced plasmas

## Examples applications

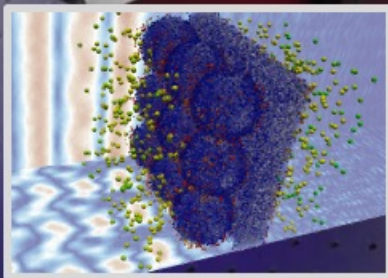
Simulation techniques  
in hot plasma modeling



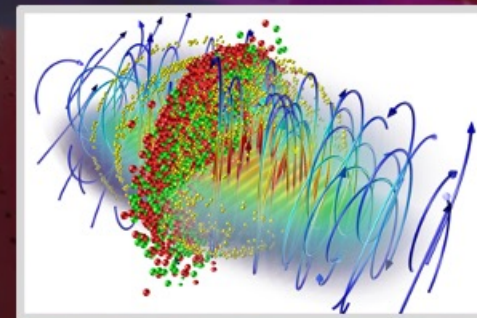
electron beam acceleration



generation of energetic radiation



ion beam acceleration



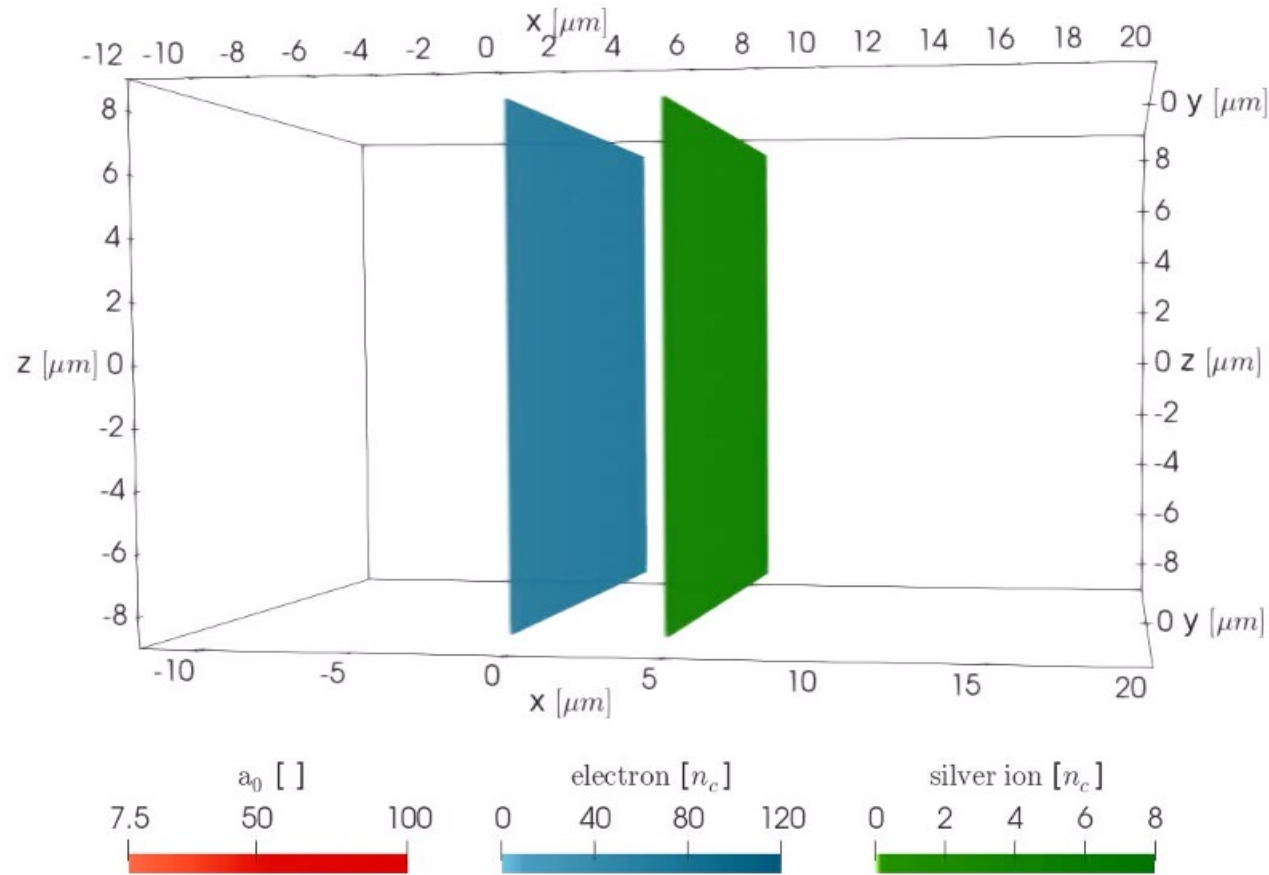
electron-positron pair production



# Particle methods for laser-produced plasmas

## Examples applications

Simulation techniques  
in hot plasma modeling



Plasma shutter for improved  
heavy ion acceleration  
by ultra-intense laser pulses

M. Matys, S. V. Bulanov, M. Kucharik,  
M. Jirka, J. Nikl, M. Kecova, J. Proska,  
J. Psikal, G. Korn and O. Klimo

# Particle methods for laser-produced plasmas

## Examples applications – ICF related


Simulation techniques  
in hot plasma modeling

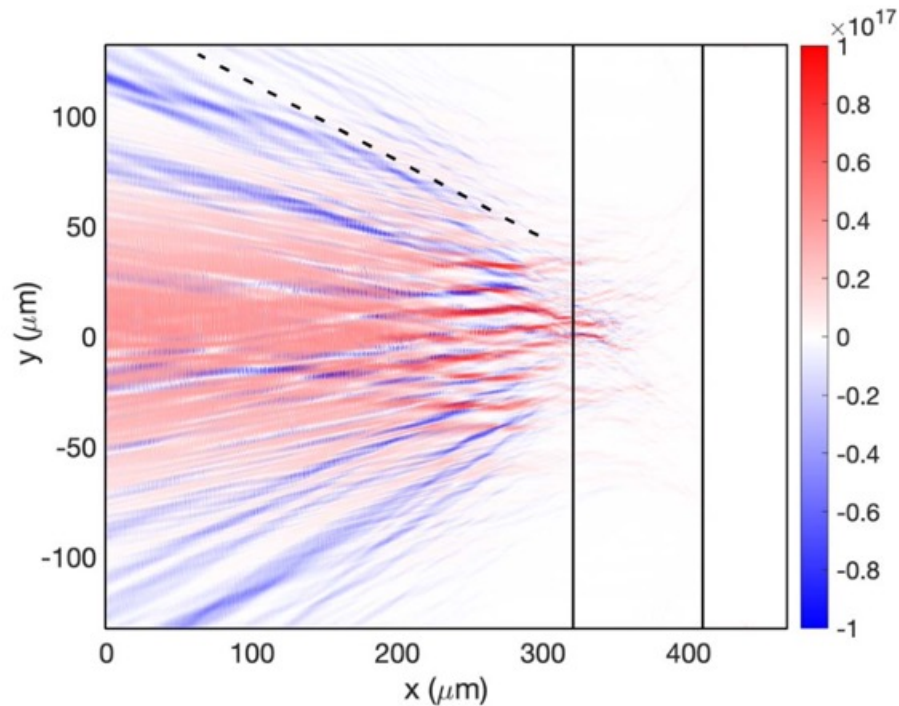
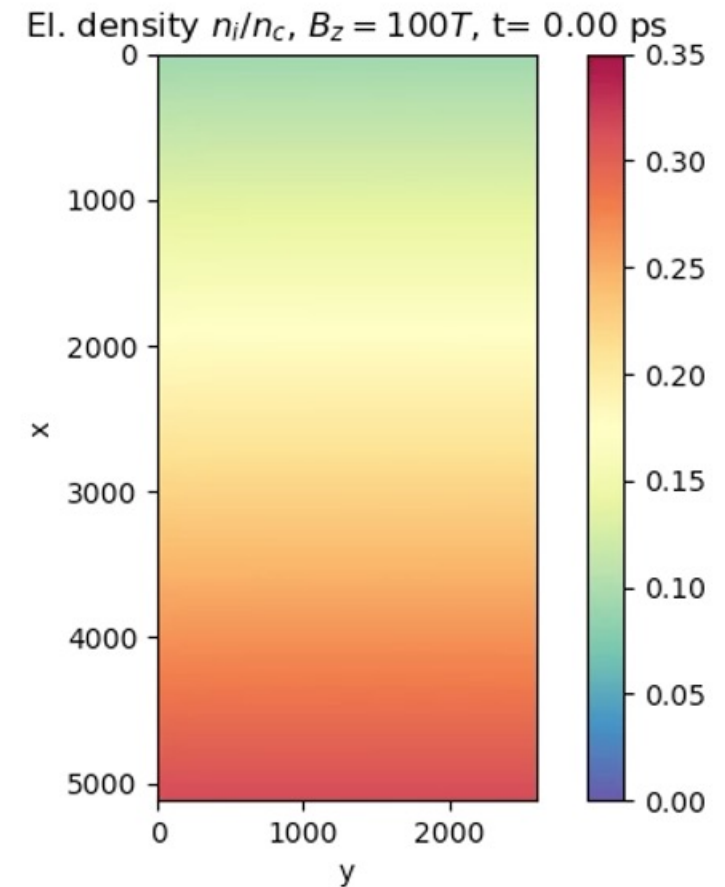
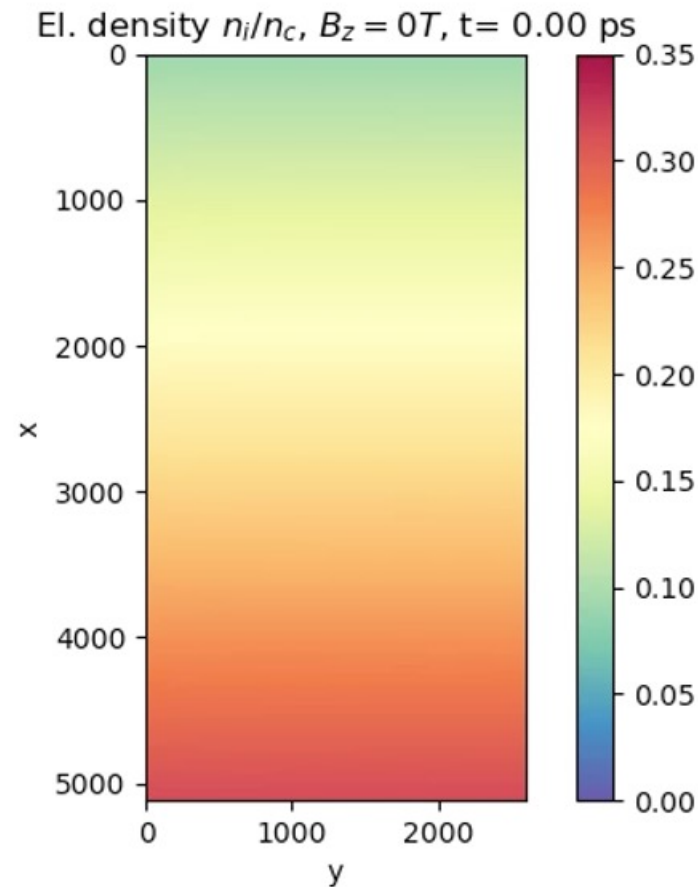


**Figure 9.** Distribution of the Poynting flux in the laser propagation direction (in units  $\text{W} \cdot \text{cm}^{-2}$ ) averaged temporally over 3 ps during the quasi-steady stage of interaction and spatially over one laser wavelength. Red and blue colours represent therefore incident and backscattered light, respectively. The incident laser beam is propagating from the left and the black vertical lines show the position of the quarter critical and critical density surfaces. The black dashed line is shown to guide the eye for the opening angle of backward propagating light.







# Particle methods for laser-produced plasmas

---

doc. Ing. Ondřej Klimo, Ph.D.  
FJFI CTU in Prague, ELI ERIC  
ondrej.klimo@fjfi.cvut.cz

What was not covered here?

- Particle-in-cell simulation method for macroscopic degenerate plasmas  
<https://doi.org/10.1103/PhysRevE.102.033312>
- The Pretty Efficient Parallel Coulomb Solver  
<https://www.fz-juelich.de/en/ias/jsc/about-us/structure/simulation-and-data-labs/sdl-plasma-physics/pepc>

## Thank you for attention